

CHALMERS



Validation of VTT Model in Predicting Permanent Deformation

A Study on the Permanent Deformation Behaviour of Unbound Granular Material in Flexible Pavements

Master of Science Thesis in Geo and Water Engineering Department

YANING QIAO

Department of Civil and Environmental Engineering

Division of Geo Engineering

Road and Traffic Group

CHALMERS UNIVERSITY OF TECHNOLOGY

Gothenburg, Sweden 2010

Master's Thesis 2010:147

MASTER'S THESIS 2010:147

Validation of VTT Model in Predicting Permanent Deformation

A Study on the Permanent Deformation Behaviour of Unbound Granular Material in
Flexible Pavements

Master's Thesis in Geo and Water Engineering

Yaning Qiao

Department of Civil and Environmental Engineering

Division of Geo Engineering

Road and Traffic Group

CHALMERS UNIVERSITY OF TECHNOLOGY

Gothenburg, Sweden 2010

Validation of VTT Model in Predicting Permanent Deformation
A Study on the Permanent Deformation Behaviour of Unbound Granular Material in
Flexible Pavements
Master's Thesis in Geo and Water Engineering
YANING QIAO

© YANING QIAO, 2010

Examensarbete / Institutionen för bygg- och miljöteknik,
Chalmers tekniska högskola 2010:147

Department of Civil and Environmental Engineering
Division of Geo Engineering
Road and Traffic Group
Chalmers University of Technology
SE-412 96 Gothenburg
Sweden
Telephone: + 46 (0)31-772 1000

Cover:

Pictures are triaxial test apparatus from SINTEF laboratory in Norwegian Institute of
Technology (NTNU) in Trondheim, Norway and road investigation in Nässjö,
Sweden taken by Yaning Qiao.

Chalmers Reproservice /Department of Civil and Environmental Engineering
Gothenburg, Sweden 2010

Validation of VTT Model in Predicting Permanent Deformation
A Study on the Permanent Deformation Behaviour of Unbound Granular Material in
Flexible Pavements
Master's Thesis in the Geo and Water Engineering Program
YANING QIAO
Department of Civil and Environmental Engineering
Division of Geo Engineering
Road and Traffic Group
Chalmers University of Technology

Abstract

Rutting is a very common type of flexible pavement distress all over the globe. A rut originates as permanent deformation on low volume traffic road, attributing greatly to repeated traffic load. It may cause uncomfortable driving experience or even danger to road users. Consequently it is greatly taken care of in the Pavement Management System (PMS).

Prediction of future rutting is one of the countermeasures to the rutting problem and can elicit solutions for reducing cost on road maintenance and improving traffic safety. There have been many studies about the pavement rutting problem and plenty of models have been developed for predicting future rutting. These models can be categorized as empirical, mechanical or empirical-mechanical. As the development of finite element (FE) program, many models are able to take material behaviour such as nonlinearity and anisotropy into consideration and these models are thus more sophisticated to a certain degree. However, the real rutting is affected by so many factors, such as weather condition, field moisture, local landscape and nonlinearity and anisotropic properties of the material that are beyond the predictability of many models, hence the bias between the predicted rutting depth and the real rutting depth exists.

VTT model is a model to simulate the permanent deformation behaviour in unbound granular materials. This model is developed in Finland and during this work, it is planned to be validated applicable for some roads in Sweden. Repeated loading triaxial (RLT) test is performed for samples taken from the unbound granular layers (UGLs) of the investigated roads. VTT model is validated with the knowledge of the result from RLT tests. By implementing VTT model into the permanent deformation prediction tool VägFEM, permanent deformation on investigated road are calculated and compared with measured rutting and prediction from Gidel model.

Key words: Permanent deformation, unbound granular material, validation, VTT model.

Contents

1	INTRODUCTION	1
1.1	Aim	2
1.2	Limitation	2
1.3	Method	3
2	SITE DESCRIPTION	4
2.1	Information about Rv E6, Dingle	4
2.2	Information about Rv 31, Nässjö	5
2.3	Information about Rv 46, Trädet	6
2.4	Sample conditions and assumptions	7
3	LITERATURE REVIEW	9
3.1	Flexible pavement structure	9
3.2	Elastic and plastic deformation of a pavement	10
3.3	Rutting and rutting mechanics	10
3.4	Shakedown concepts	11
3.5	Deformation behaviour of unbound granular material in different ranges	12
3.5.1	Mechanics in different shakedown range	12
3.5.2	Evaluation of shakedown range	13
3.6	Factors affecting plastic deformation	13
3.6.1	Number of loading cycles	14
3.6.2	Moisture content	14
3.6.3	Degree of compaction	14
3.6.4	Density	14
3.6.5	Grading	14
3.6.6	Stress history	14
4	PERMANENT DEFORMATION CALCULATION MODEL	15
4.1	Total Permanent deformation calculation	15
4.2	Permanent deformation models for different layers	16
4.2.1	Permanent deformation model for asphalt layer	16
4.2.2	Permanent deformation model for unbound granular layer	16
5	VTT MODEL, MMOPP MODEL AND GIDEL MODEL	18
5.1	VTT Model	18
5.1.1	Shear yielding	18
5.1.2	VTT model parameters	19
5.2	MMOPP model	20

5.3	Gidel model	22
6	REPEATED LOAD TRIAXIAL (RLT) TEST	23
6.1	Preparation of the specimen	23
6.2	Deviatoric pressure and confining pressure	23
7	RESULT	25
7.1	Shakedown range evaluation	25
7.2	Regression factor calibration	27
7.3	Permanent deformation calculation	29
7.3.1	Rutting calculation for Dingle and comparison	29
7.3.2	Rutting calculation for Nässjö and comparison	30
7.3.3	Rutting calculation for Trädet and comparison	31
8	SENSITIVITY ANALYSIS	33
8.1	Sensitivity analysis for rutting prediction model implemented with VTT model	33
8.2	Result	34
9	DISCUSSION	35
10	CONCLUSION AND RECOMMENDATION	36
11	REFERENCES	37
12	APPENDIX	39
12.1	Appendix 1	40
12.2	Appendix 2	65
12.3	Appendix 3	68
12.4	Appendix 4	69
13	LIST OF FIGURES	72
14	LIST OF TABLES	74

Preface

This work echoes the course “Master’s thesis in Civil and Environmental Engineering (course code: BOMX02)” at Civil and Environmental Engineering Department at Chalmers University of Technology, Sweden. The thesis work started from March 2010 and completed until October 2010.

This work belongs to a research project called “NordFoU” which has been made under cooperation among Nordic countries. The project level of NordFoU project named “Performance Prediction Models for Flexible Pavements” is executed at Trafikverket (Traffic Administration) in Västra Götaland, Sweden. The work is a part of Performance Prediction Models for Flexible Pavements.

This work has been carried out with supervision from Anders Huvstig from Trafikverket and Associate Professor Gunnar Lannér from Chalmers University of Technology as advisors. During the work, Professor Inge Hoff from Norwegian Institute of Technology (NTNU) and Professor Leena Korkiala-Tanttu from Helsinki University of Technology offered numerous help by answering my questions on specific technical and practical areas. My colleague Johan Afseer and Kenneth Svensson helped me a lot in particular technical aspects and Swedish language. I owe all of them my sincere thanks!

At last, although not the last thing to mention, the work will never be performed without the dedication of the laboratory staff at SINTEF, Norway and SKANSKA, Sweden. I appreciate their earnest academic attitude and their immense contributions.

Gothenburg, October 2010

Yaning Qiao

Notations

A, B, C	MMOPP model factors
a1, a2	Asphalt layer permanent strain model factors
b, C	VTT Model factors
CBR	California Bearing Capacity
D1	Base layer of Dingle
D2	Subbase layer of Dingle
D3	Subgrade of Dingle
DOC	Degree of compaction
ESAL	Equivalent Single Axle Load
F(t)	Function with parameter t
FE	Finite Element
FWD	Falling Weight Deflectometer
h_n	Thickness
HVS	Heavy Vehicle Simulator
L_{max}	Gidel model parameter
LTTP	Long Term Pavement Performance
m, s	Parameters of the failure line of the material
N	Number of load cycles
N1	Base layer of Nässjö
N2	Subbase layer of Nässjö
N3	Subgrade of Nässjö
p	Mean value of principal stress
p_a	Reference pressure (100 kPa) in Gidel model
PD_i	Permanent deformation in layer i
p_{max}	Maximum mean value of principal stress
PMS	Pavement Management System
q	Deviatoric stress
q_c	Deviatoric stress for plastic creep limit
q_f	Deviatoric stress at failure of the material
q_{max}	Maximum deviatoric stress
q_s	Deviatoric stress for plastic shakedown limit
R	Failure ratio in VTT model
RLT	Repeated Load Triaxial
S	Relative value for sensitivity

T	Temperature
t	Parameter in sensitivity model
T1	Base layer of Trädet
T2	Subbase layer of Trädet
T3	Subgrade of Trädet
UGM	Unbound Granular Material
UGMs	Unbound Granular Materials
UGL	Unbound Granular Layer
UGLs	Unbound Granular Layers
ε_p	Permanent axial strain
ε_1^{p0}, B, n	Gidel model factors
$\varepsilon_{3000}, \varepsilon_{5000}$ test	Permanent strain at pulse 3000 and 5000 of the repeated load triaxial test
ε_r	Resilient strain
σ_1	the major principal (vertical) stress
σ'	reference stress (atmospheric pressure, 0.1 Mpa)
σ_c	Confining pressure imposed in repeated load triaxial test
σ_d	Deviatoric pressure imposed in repeated load triaxial test
$\Delta F(t)$	Increment in function of sensitivity model
Δt	Increment in parameter of sensitivity model

1 Introduction

In 2004, Nordic countries (Norway, Sweden, Denmark, Finland and Iceland) initiated the NordFoU cooperation program for road authorities in the area of road research and development.

The pavement performance model is one project carried out under the NordFoU program with the aim to predict future performance and deterioration of flexible pavements, to evaluate different performance models and to validate those models for each country. By collaborating the study and research, each Nordic country is able to improve present prediction tools, to achieve more effective road asset management, to perform better assessment of road maintenance and operation cost and to reduce the cost both in construction phase and maintenance phase.

In different categories of pavement performance, the permanent deformation behaviour of unbound granular material (UGM) remains to be a problem which has not been successfully handled for many decades because of the complexity of the material and its plastic behaviour which is difficult to describe in a certain material model. Scientists have tried to build up the mechanic-empirical models to simulate the permanent deformation behaviour in the UGLs and many of those models are capable of solving the problems well locally. However, those models might not be applicable in an altered environment. So it is always essential to validate the model when the material model is applied in altered condition.

VTT model is a Finnish model developed by Korkiala-Tantu (2009) to describe the permanent deformation in unbound granular layer (UGL). During the work, the VTT model is going to be validated and later implemented into the Swedish Pavement Management System (PMS) tool called VägFEM as an option for predicting rutting depth. The prediction by VTT model will subsequently be compared with real measured rutting and prediction from another model called Gidel model in order that the performance of VTT model can be evaluated with some recommendations proposed at last.

The validation of VTT model is performed in three chosen locations in Sweden (Dingle, Nässjö and Trädet) because of the availability of the properties of the roads. Triaxial tests have been performed on samples taken from layers of those roads. The information of these roads has been stored in the Swedish Long Term Performance Pavement (LTPP) database although the data are not always completely sufficient.

1.1 Aim

The aim of this work is to validate the Finnish VTT model applied to three investigated Swedish roads and implement this material model into Swedish PMS (VägFEM). The performance of VTT model is going to be compared with Gidel model and the rutting depth by measurement. In the dissertation, the following questions are going to be answered:

- How can the Finnish VTT model be validated in three selected roads from Sweden?
- How good is the prediction of rutting by VTT model compared with Gidel model as well as the real measured rutting?
- Which parameter in VTT model is the most sensitive one and has larger effect on rutting prediction?

1.2 Limitation

Rutting on a pavement has been categorized into different types. While in cold climate areas and low volume traffic roads (e.g. many roads in Sweden), permanent deformation in pavement accounts for most probable category of rutting. So in this dissertation, the term “Rutting” and “Permanent deformation” are deemed to be identical concept.

In general, this dissertation discusses permanent deformation in pavement while there is an emphasis on permanent deformation behaviour in unbound granular materials (UGMs) and the model to describe it, especially the Finnish VTT model.

There has not been comprehensive data for all layers from the three investigated roads. For those layers without intact data describing the properties, material properties will refer to similar known layers.

Although there are some differences between cumulative equivalent single axle load (ESAL) and number of loading repetitions, when calculating the permanent deformation by VTT and Gidel model, the number of loading repetitions are replaced by the value of cumulative ESAL.

1.3 Method

The method and the procedure of this thesis can be concluded in four steps:

1. Shakedown range analysis
2. Model factor calibration
3. Permanent deformation calculation
4. Sensitivity analysis

Shakedown range analysis

Several samples from different UGLs are collected from three investigated road sections in Sweden. These samples were delivered to laboratory where triaxial tests were made. By using the triaxial test result, permanent deformation behaviour in those Swedish materials can be studied. One important target of doing the triaxial tests is to analyse the shakedown range of the material. By the analysis of shakedown range, the relation between the behaviour of UGMs and stress state in those layers can be revealed. Another target of shakedown range analysis is to exclude the triaxial data at high stress level which could not be used in factor calibration of VTT model.

Model factor calibration

The triaxial tests also give hints about how number of loading cycles correlate to the rutting depth. With triaxial data on number of loading cycles and stress state, permanent deformation in these samples can be calculated with VTT model. The calculated permanent deformation can then be compared with measured deformation in these samples from triaxial tests to back calculate the factors for VTT model by regression method.

Permanent deformation calculation

With a validated VTT model, the permanent deformation in UGLs can be calculated. At the same time, the permanent deformation in other layers other than UGLs can be obtained from existing models. By summing up the deformation in all layers, the total rutting depth on the pavement can be calculated (The calculation will be solved automatically by VägFEM with inputted parameters). Those values will be compared with the prediction from Gidel model and the real rutting measurement. Final conclusion will be the evaluation on VTT model subsequent to the comparison.

Sensitivity analysis

Sensitivity analysis is performed to learn which parameter in VTT model has largest effect on the rutting depth. Besides, other parameters from permanent deformation model such as the static failure properties of the UGM are studied as well.

2 Site description

There are three roads that are investigated by Trafikverket, Västra Götaland, Sweden, as a part of the performance prediction model. Several samples have been taken from different layers in these roads and have been evaluated by laboratory tests. The investigated roads are:

- Rv E6 Dingle
- Rv 31 Nässjö
- Rv 46 Trädet

All these three roads belong to the Swedish LTPP database. Information about the road such as geometry, material, traffic volume and condition of the road for example rutting and cracks are monitored. The information has been stored in a form which is recognizable and applicable by FE tool VägFEM.

Measurement such as rutting depth has been done for these locations by a laser equipped car (RST). The measurement data are available in LTPP database.

2.1 Information about Rv E6, Dingle

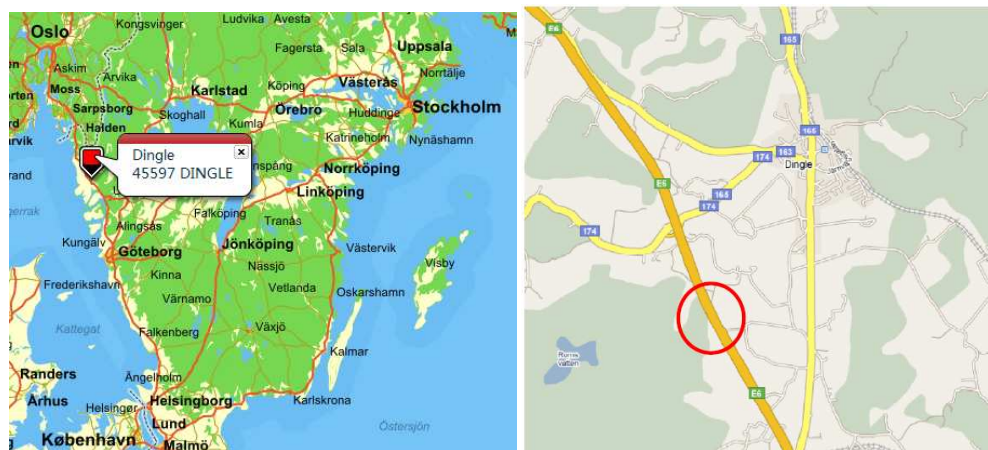


Figure 2.1 Location of Dingle and road Rv E6 (Huvstig 2009).

Dingle locates on the west coast of Sweden. Tested section of road Rv E6 is several kilometers in the west of Dingle. Rv E6 has been built from 1998 and operated since the spring of 2000. The road has been used as a motorway with two driving lanes and outer shoulders, adding up to nineteen meters. Agricultural farm lands are the common landscape mostly expected along the road.

Table 2.1 Layer information of tested section, Rv E6, Dingle (Huvstig 2009).

Layer	Thickness mm	Material	Year
Wearing course	35	ABS 11 (B85)	2000
Third asphalt layer	45	ABb 16 (Binding layer, B180)	1999 – 2000
Second asphalt layer	40	AG 16 (Bituminous bound base, B180)	1999 – 2000
First asphalt layer	50	AG 22 (Bituminous bound base, B180)	1999 – 2000
Base	80	Crushed rock: VÄG 94	1998 – 99
Sub base	1200	Crushed rock: VÄG 94 (0 – 200 mm)	1998 – 99
Subgrade		Clay	

The triaxial test has only been done with the UGM in base layer. The measured density of the UGM is 2.35 g/cm^3 . The high value of density indicates the contribution to compaction from the abundant traffic loading. From the investigation of the road in the year 2008, it is discovered that the rutting has been unexpectedly large. The measured rutting can arrive at a depth of 20 mm by the year 2008.

2.2 Information about Rv 31, Nässjö

The city of Nässjö locates in the county of Jönköping, Sweden. It is about 50 kilometers southeast of Jönköping.



Figure 2.2 Location of Nässjö and road Rv 31 (Huvstig 2009).

The tested road is Rv 31, southeast of Nässjö. It was constructed between the year 1987 and 1988 and operated since September, 1988. The road is located within a forest landscape. Road Rv 31 is divided into eleven sections and the length of each section is a hundred meters. Section number 6 and 9 were chosen for testing. The width of driving lanes is 7.5 m and the length of the shoulder is 0.25 m on each side.

Table 2.2 Layer information of section 6S and 9S, Rv 31, Nässjö (Huvstig 2009).

Layer	Thickness mm	Material	Year
Wearing course	24	Hot remixing plus 60ABS16 (New wearing layer)	2007-08-10
Second asphalt layer	35	80MABT16 (Wearing layer)	1989-07-01
First asphalt layer	50	110AG (Bituminous bound base)	1988-11-01
Base	115	Gravel base material: BYA 6:06	1988
Sub base	500	Gravel of class A: BYA 6:03	1987-88
Subgrade		Silty moraine, class 6 (Frost class III)	

About eight years later in the maintenance, a wearing course was installed to improve the surface performance. The dry density of the base material is 2.25 g/cm^3 on section 6S and 2.22 g/cm^3 on section 9S. On section 6S, the moisture content is 1.9 % under the base surface and on section 9S, the moisture content is 1.96 %. It is observed on section 6S, the rutting depth reached 19.3 mm in the year 2007 and on Section 9S, this number is 13.0 mm.

2.3 Information about Rv 46, Trädet

The road Rv 46 is located to the north of Trädet. The road is divided into nine 100 m sections.



Figure 2.3 Location of Trädet and road Rv 46 (Huvstig 2009).

The road was built from 1985 to 1986 and has been opened for traffic since November, 1986. A second asphalt layer and a wearing course have been added after that.

The road was built within an agricultural landscape with two driving lanes which are 7.5 m in total. Shoulders which are 0.25 m were installed on each side of the road.

Table 2.3 Layer information of section 4, Rv 46, Trädet (Huvstig 2009).

Layer	Thickness mm	Material	Year
Wearing course	0	Y1B16 (Surface treatment)	1988-07-01
Second asphalt layer	12	MaJu30MABT12 (Adjustment layer)	1987-07-01
First asphalt layer	70	165AG (Bituminous bound base)	1986
Base	125	Gravel base material: BYA 6:06	1986
Sub base	410	Gravel of class A: BYA 6:03	1986
Subgrade		Friction material, class I (Frost class I)	

The dry density of the base material is 2.42 g/cm^3 and the moisture content is 1.8 %. The measurement of rutting shows depth of 4.3 mm on section 4 and 13.5 on section 5.

2.4 Sample conditions and assumptions

Triaxial tests have not been done with D2, D3, T2 thus there are not enough data for these layers. In the later calculation, the missing area is dealt by the assumption below the table.

Table 2.4 Sample condition (Hoff 2009).

Road	Layer	Dry density (g/	Moisture
Rv E6 Dingle	Base (D1)	2.35	1.96
	Subbase (D2)	-	-
	Subgrade	-	-
Rv 31 Nässjö	Base (N1)	2.25	1.85
	Subbase (N2)	2.25	4.00
	Subgrade	2.02	8.00
Rv 46 Trädet	Base (T1)	2.42	1.80
	Subbase (T2)	-	-
	Subgrade	1.90	7.00

Samples for triaxial tests have been collected from three locations in different UGLs. Although for some UGLs of the selected road, no sample is collected for triaxial tests (D2, D3 and T2). Thus the material properties can be obtained only by assumption. The assumptions are made as follows:

1. D2 and D3 are the same as D1 because of the similarities in the material used in Dingle.
2. The material used in T2 is comparable to N2 thus the properties in N2 can be used to model the performance of T2.

Samples from base layer in the three roads and subbase layer from Nässjö were sent to laboratory (SINTEF) at Norwegian Institute of Technology (NTNU), Norway and triaxial tests were performed on those samples. Samples from subgrade in Nässjö and Trädet were taken and their RLT tests were made by Skanska, Malmö, Sweden.

3 Literature review

Flexible pavements have been used for many years as the most common pavement type in different parts of the world and under diverse climate conditions. The advantage of flexible pavements such as comfort while driving and easy for maintenance adds bonus to its superiority compared to rigid pavement structure. However there are some disadvantages and rutting is one of them.

3.1 Flexible pavement structure

A flexible pavement structure can be described as a “Multi-layer” system. Permanent deformation can take place in all layers of a pavement. A typical flexible pavement profile consists of five layers (Huang 2004):

Bituminous surface layer: The bituminous surface layer is the top layer of the pavement structure which consists of up to 40 mm of bitumen which is durable to resist the abrasion and traffic load. It is the most expensive layer of a pavement structure and will withstand highest stress.

Bituminous bound layer: Beneath the bituminous surface layer, the bituminous bound layer consists of mixtures of bitumen and granular material which is stable and can transmit the traffic load downwards. The bituminous bound layer can be around 170 mm thick.

Unbound base layer: The unbound base layer is made of approximately 80 mm of unbound granular material placed below the bituminous bound course. The traffic load will transmit to the layer beneath.

Subbase layer: The subbase layer lies under the unbound base layer. It consists of about 700 mm of unbound granular material where local material can be used.

Subgrade: The subgrade is the in-situ material which is compacted to a certain density and moisture content.

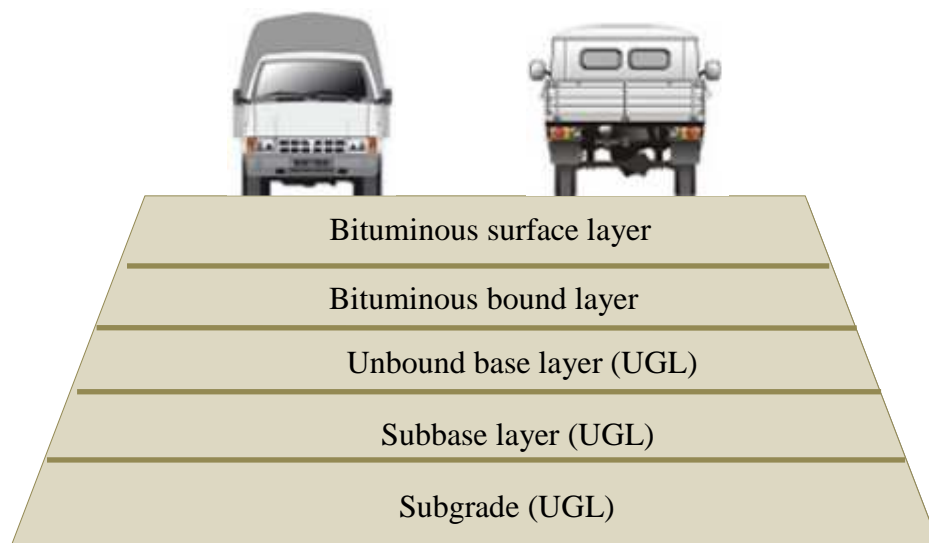


Figure 3.1 Multi-layer system of a pavement.

Unbound base layer together with subbase layer and subgrade belong to UGL, as the name has told, because they are all made of granular material without bindings.

3.2 Elastic and plastic deformation of a pavement

When a pavement is loaded with traffic, deformation will occur at different layers of the pavement. Generally speaking, about the deformation of a pavement, one can always refer to two types of deformation mechanisms as normally described in material mechanics:

Elastic deformation

When a pavement structure is loaded with traffic, there is one part of deformation which will vanish after unloading. This type of deformation is called elastic deformation and it is totally resilient. The resilient behaviour will occur when the level of applied load is low.

Plastic deformation

Plastic deformation is also called permanent deformation. It will occur in all different layers of pavement structure. Plastic deformation will take place when the applied stress is high enough. Plastic deformation is the deformation which is unrecoverable after unloading. It is the main reason for rutting in cold climate conditions under low volume traffic.

3.3 Rutting and rutting mechanics

Rutting appears as depression on the surface of a pavement (Figure 3.2). It is apparent after precipitation where a pool of water can be found on the pavement. Rutting has very complicated mechanisms and it could generate in many different ways. Abrasion from studded tires, weak subgrade and permanent deformation in pavement structure can all contribute to the growth of a rut. In countries like Sweden with low volume of traffic, the major concern is from the permanent deformation that occurs in different layers of the pavement structure. This dissertation is limited to describe rutting which is caused by permanent deformation in the pavement structure.



Figure 3.2 A picture illustrating a rut (PCA 2010).

As rutting may cause damage to the road and it is potentially dangerous to the road users, PMS has taken this into consideration and the rut is measured as a part of the

maintenance work. Generally, there are two ways of measuring a rut. The first and conventional one is called “beam method” where a beam is used as reference to measure the gap between top and bottom of a rut. Nowadays, as the development of electronic devices and laser technology, there has been a new method “RST car” rutting measurement which is applied by equipping several laser sensors to the testing car and they will record the elevation of the beaten road in form of section profiles. The rutting depth can be analysed from the laser recordings.

For the bituminous surface layer and bituminous bound layer, there has been accurate and precise model for predicting their permanent deformation behaviour. While for UGLs, a lot of researches have been done and plentiful models have been set up. For most of the UGM models, they have a common basis which is called the concept of shakedown, describing structures’ permanent behaviour under repeated loading.

3.4 Shakedown concepts

The shakedown concept is widely adopted in describing the deformation behaviour of materials under repeated loading. At first, the shakedown concept was introduced here to describe the behaviour of the metal surface under repeated loading and then it is introduced to describe permanent deformation behaviour of UGM under repeated traffic loading.

When a pavement has been open for traffic, loading caused by traffic acts as repeated loading which is imposed on the pavement surface. The upper asphalt layers deliver the loadings to the UGLs so that the UGMs will also be under repeated loading.

Many studies have revealed that shakedown behaviour exists in UGMs as a consequence of the repeated traffic loading. Dawson et al. (1999) advised to make use of the RLT data in plotting the vertical permanent strain rate and permanent vertical cumulative strain. The result shows that the data are clearly sorted in three ranges.

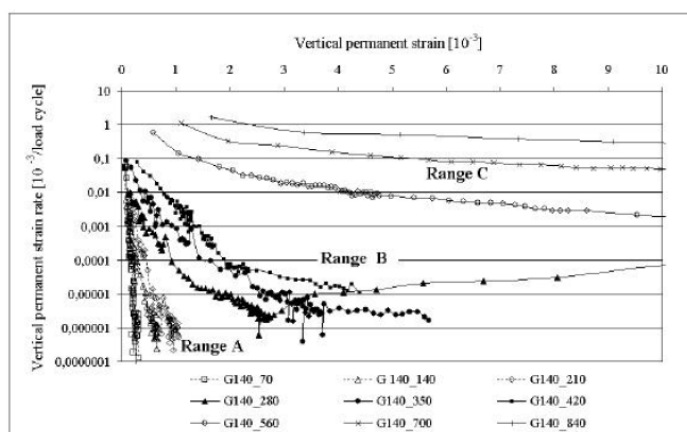


Figure 3.3 Clearly sorted shakedown range by plotting vertical permanent strain rate and vertical permanent strain (Werkmeister 2003-1).

According to Werkmeister (2003-2), the behaviour of a certain material under repeated loadings can be described in three different deformation categories: plastic shakedown range (Range A), plastic creep range (Range B) and incremental collapse (Range C).

Generally speaking, the shakedown range of the UGM will be determined by the imposed loading and material properties. As shown in the figure above, Range A takes place when UGM is under plastic shakedown-limit with low loading stress level. As load increases, UGM will experience plastic creep behaviour. While the loading exceeds the plastic creep limit, incremental collapse will occur in UGM.

3.5 Deformation behaviour of unbound granular material in different ranges

In different ranges of shakedown concept, the behaviour of UGM differs both in macro and micro perspectives. The most common way to show differences among shakedown ranges is to make use of the RLT tests result and plot the accumulated plastic strain versus number of loading cycles.

3.5.1 Mechanics in different shakedown range

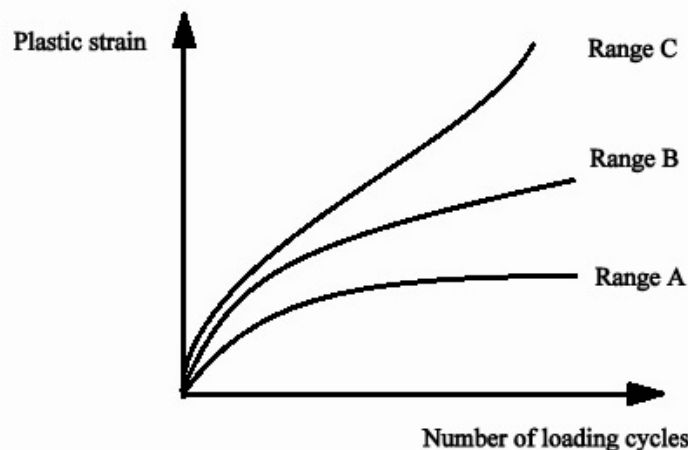


Figure 3.4 Shakedown ranges plotted on a ϵ_p versus N diagram.

Range A

The granular material experiences low level of stress which will lead to a phase of initial post-compaction. The disordered granular material will be re-oriented and some will break due to the loosen structure. During this phase, particle attrition will come about while it is not significant.

In the phase of initial post-compaction, the accumulation of permanent strain is faster compared with the following phase which is characterized by a linear log (ϵ_p) versus log (N) plot.

On a plotted number of loading cycles versus plastic strain diagram from RTL test, plastic strain of UGM in Range A will almost stop to propagate after a number of loading repetitions. The permanent deformation is plastic during the first finite number of loading cycles then the deformation behaviour becomes totally resilient.

Range B

When the imposed stress is higher, the permanent deformation of UGM will behave as in Range B. The accumulation of strain is faster under Rang B compared to Range A during a finite number of loading cycles. After that, the strain accumulates in a constant rate.

An effect of recoverable particle rotations and of additional recoverable slip between particles is a characteristic micromechanical phenomenon occurs only in Range B (Werkmeister 2003-3).

Grain attrition is believed to be a main reason for the collapse of UGMs (Werkmeister 2003-3). At high stress, the volume increase caused by dilatation of the material is another reason for collapse (Hoff 1999-1).

Range C

Whilst the imposed stress level is high enough, the UGM will collapse. The permanent deformation from Range C initializes from a primary creep phase by a post-compaction period which is similar to Range A and B. However the strain accumulates much faster. Afterwards the second creep will take place, followed by tertiary creep. Both grain abrasion and particle crushing may occur in Range C (Werkmeister 2003-3).

3.5.2 Evaluation of shakedown range

The RLT tests can be used in determining material parameters such as resilient modulus, shakedown range and so on.

Shakedown range analysis

It is necessary to know the shakedown range of the UGM in the three selected road. Because by calculating the shakedown range of the UMG, one can build up the model for the permanent deformation in those granular layers in mathematical ways. Korkiala-Tanttu (2009-1) has proposed the VTT model for permanent deformation calculation for UGMs, this model can be adjusted in the same mathematical way into the selected Swedish road.

The evaluation of shakedown range for UGMs is done according to Werkmeister's theory on the shakedown concept and shakedown range of the UGMs. A method using triaxial data to determine the shakedown range was proposed (Werkmeister 2003-4):

$$\varepsilon_{3000} - \varepsilon_{5000} < 0.045 * 10^{-3} \quad \text{Range A} \quad (\text{Eq. 3.1})$$

$$0.045 * 10^{-3} < \varepsilon_{3000} - \varepsilon_{5000} < 0.4 * 10^{-3} \quad \text{Range B} \quad (\text{Eq. 3.2})$$

$$\varepsilon_{3000} - \varepsilon_{5000} > 0.4 * 10^{-3} \quad \text{Range C} \quad (\text{Eq. 3.3})$$

Where ε_{3000} and ε_{5000} (10^{-3}) are the plastic strain when loading cycles equal to 3000 and 5000 in RTL tests.

3.6 Factors affecting plastic deformation

The permanent deformation of UGM is affected by a variety of factors including internal factors and external factors. Although the plastic deformation behaviour is

complicated, the existing models are able to describe the reality well to some extent. Factors that affect permanent deformation in UGM can be concluded as follows.

3.6.1 Number of loading cycles

The permanent deformation is strongly related to the number of loading cycles and its importance has been magnified by the power b (Eq. 4.4). The number of loading cycles corresponds to the cumulative equivalent single axle load, suggested by VägFEM program. The real situation is that the number of loading cycles always needs to be combined with the stress of each load.

3.6.2 Moisture content

The moisture content alters the mechanical properties of the UGMs. As there is always water existing in the UGMs, the water will form film and affects on the shear resistance between grains. The optimum moisture content comes about when the dry density reaches the maximum value. When optimum moisture content has been reached, the UGM is suppose to have maximum bearing capacity in resisting permanent deformation and shear yielding.

3.6.3 Degree of compaction

The degree of compaction (DOC) and moisture content reaches the optimum value at the same time. The UGLs are compacted during construction. The UGM will gain best ability to resist against axial permanent deformation, resilient deformation as well as shearing yielding. So the DOC is always a critical qualification indicator of a good road.

3.6.4 Density

Density of the UGM can affect the permanent deformation behaviour. Generally speaking, larger density will result in better resistance towards permanent deformation.

3.6.5 Grading

Resistance towards permanent deformation increases with more fine contents (Ekblad 2004). Also the maximum grain size affects permanent deformation. UGM will have lower deformation if the maximum grain size is bigger (Hoff 1999-2).

3.6.6 Stress history

Stress history directly affects permanent deformation behaviour of UGMs. When UGMs have been exposed to rather low stress history, the permanent deformation could be bigger than common. In the other way, if UGMs has been imposed to high stress history, the permanent deformation will probably be smaller.

4 Permanent deformation calculation model

Rutting accumulates as plastic deformation in each layer of the pavement structure and appears on the surface of a pavement. The permanent deformation model consists of material model of asphalt layers and material model of UGLs. The material model of permanent deformation behaviour from asphalt layers and granular layers differs from each other.

In a perspective of material science, the asphalt layers including bituminous surface layer and bituminous bound layer present semi-solid and viscous properties thus it is highly affected by the temperature while temperature has much less effect in granular layers.

4.1 Total Permanent deformation calculation

The total rutting is calculated by summing up the permanent deformation in all the layers, including deformation in the asphalt layers, base layer, subbase layer and subgrade.

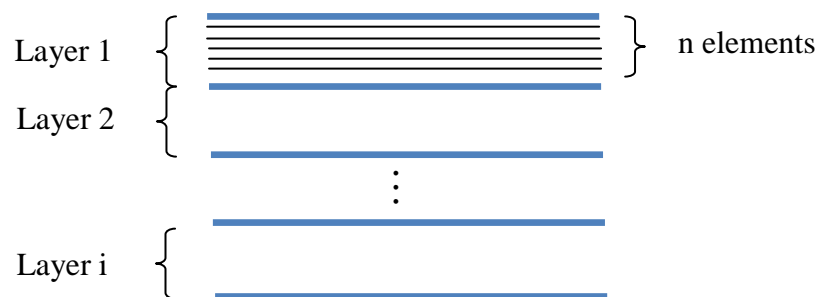


Figure 4.1 the multi-layer model for calculating rutting depth.

In each layer, the depth is divided into finite thickness element (n) from the top to the bottom of the layer. The permanent deformation in each layer is calculated by sum the permanent deformation in each thickness element. The permanent deformation in layer i can be expressed as:

$$PD_i = \sum_{n=1}^n \varepsilon_n * h_n \quad (\text{Eq. 4.1})$$

where

- n number of element in a layer
- PD_i permanent deformation in layer i (mm)
- ε_n permanent strain in element layer n
- h_n thickness of element layer n (mm)

By adding the permanent deformation in different layer of the pavement, the total rutting depth can be known (Eq. 4.2).

Rutting depth:

$$PD = PD_1 + PD_2 \dots + PD_i \quad (\text{Eq. 4.2})$$

Where

PD total permanent deformation (mm)

PD_i permanent deformation in layer i (mm)

Generally speaking, the total permanent deformation on a flexible pavement can be calculated with Eq. 4.1 and Eq. 4.2. The thickness of element layer can be fixed after defining a finite number for elements wanted in a layer. What remains unknown is the plastic strain in different element layers.

4.2 Permanent deformation models for different layers

The asphalt layers could be described by one model based on semi-solid and viscous properties which is affected by temperature as well as number of loading cycles. While for UGLs, various models such as VTT model and Gidel model are introduced.

4.2.1 Permanent deformation model for asphalt layer

There has been much study on the permanent deformation behaviour in area of asphalt layers and the material model has been implemented well in real conditions. So the material model for asphalt layers is directly adopted from the standard NCHRP (2004) as follows:

$$\varepsilon_p = \varepsilon_r * a_1 * N^{a_2} * T^{a_3} \quad (\text{Eq. 4.3})$$

where

ε_p permanent strain

ε_r resilient strain

N number of load repetitions

T temperature

a_1, a_2 regression coefficients

4.2.2 Permanent deformation model for unbound granular layer

Rutting caused by permanent deformation of unbound granular material accounts for the most common damage modes for low traffic flexible pavements. In those low traffic flexible pavements, it is always the permanent deformation occurred in UGLs accounts for most rutting depth. Nowadays, there have been many studies on the material model of the unbound granular materials and a lot of models are developed such as MMOPP model, VTT model, Gidel modal and so on.

Although there are plentiful internal and external factors that decide the permanent deformation model in UGMs, only a few of those factors have principal effects. The number of loading cycles is one of the most relevant factors.

According to Korkiala-Tanttu (2009-2), a general model for plastic deformation behaviour in UGMs can be expressed as:

$$\varepsilon_p = a \cdot N^b \quad (\text{Eq. 4.4})$$

where

ε_p axial permanent strain

a, b regression parameters

N number of load cycles

Most of the UGM models are based on this general model and they include other factors into consideration respectively.

5 VTT model, MMOPP model and Gidel model

VTT model, MMOPP model and Gidel model are all permanent deformation models for UGMs. They are developed in different countries and be validated according to their own conditions. First of all is necessary to study the model and make attempt to validate these models for Swedish roads.

5.1 VTT Model

VTT (Technical Research Centre of Finland) permanent deformation model is a material model for predicting permanent deformation in UGLs. It is a nonlinear elastic-plastic model. As described in the shakedown limits of UGM by Werkmeister (2003), the behaviour of UGM under cyclic loads has three categories: plastic shakedown, plastic creep and incremental collapse which corresponding to material Range A, B and C. VTT permanent deformation model is developed on the base of the shakedown concept and can be applied in describing UGM behaviour for Range A and B but not for Range C.

5.1.1 Shear yielding

According to the study of Korkiala-Tanttu (2009-1), permanent deformation is largely affected by the shear yielding of the material. So the factor R (failure ratio) is introduced into the model. The failure ratio can be described as the ratio between deviatoric stress and deviatoric stress at failure:

$$R = \frac{q}{q_f} \quad (\text{Eq. 5.1})$$

where

q deviatoric stress (kPa)

q_f deviatoric stress at failure (kPa)

The correlation between permanent deformation and failure ratio has been proved by many researches. Regardless of the material, the vertical strain has strong correlation with failure ration R and hyperbolic function describes the correlation best.

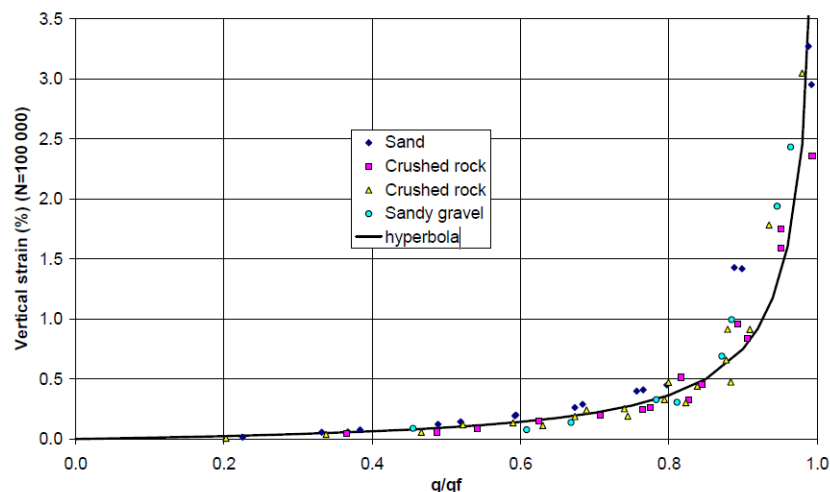


Figure 5.1 Relation between vertical strain and q/q_f (Korkiala-Tanttu L 2009-1).

Deviatoric stress at failure is measured by static triaxial tests. The linear relation between p and q_f can be shown by plots from triaxial data.

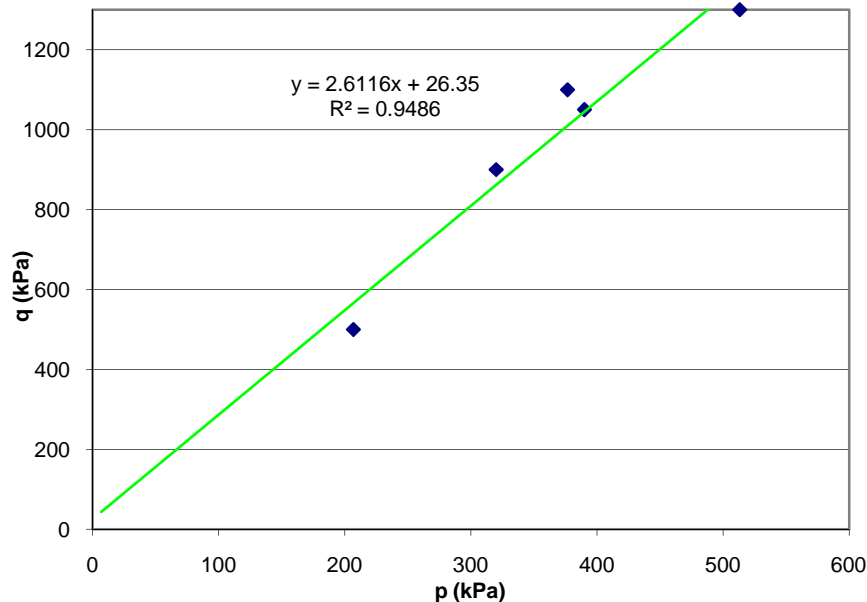


Figure 5.2 An example of static tests result (Hoff 2009). The green regression line represents the failure line of a certain UGM.

Plots by static triaxial test show the relation between p and q_f . The regression factors m and s are the gradient and intercept of the regression line. The general expression for q_f is:

$$q_f = s + m * p \quad (\text{Eq. 5.2})$$

where

q_f deviatoric stress at failure (kPa)

p mean value of principal stress (kPa)

m, s model constant

However, the relation between p and q_f is determined by the material properties such as moisture in a view of geotechnics, therefore test specimens with diverse geotechnical properties will result in different m and s .

5.1.2 VTT model parameters

As described, the permanent deformation in UGL is determined by many factors such as loading, strength of the material, moisture content, degree of compaction and so forth. While in most of the cases, it would be too complicated to take all those parameters into account. Generally, the most commonly used parameters in permanent deformation models are number of loading cycles, stress and material

strength parameters as those factors are the most sensitive factors which dominate the permanent deformation.

VTT model describes the permanent deformation as follows:

$$\varepsilon_p = C * (N)^b * \frac{R}{1-R} \quad (\text{Eq. 5.3})$$

where

ε_p permanent deformation (‰)

N number of loading cycles

R failure ratio, $R = \frac{q}{q_f}$

q deviatoric stress (kPa)

b, C model constant (regression factor in validation)

VTT model has taken number of loading cycles, stress state in the UGM and material strength of UGM into consideration.

The failure ratio R describes the ratio between the applied deviatoric loading and the deviatoric loading at failure. It takes both the applied load and material responds into consideration. The model is able to describe the permanent deformation of the UGM for shakedown range A and B, in the same word, plastic shakedown and plastic creep, but not for shakedown Range C which means the incremental collapse phase of the material.

When the applied deviatoric pressure q is closed to the failure of the material resulting $R \approx 1$, the permanent deformation will become infinity. Thus sometimes, the factor $\frac{R}{1-R}$ can be replaced by $\frac{R}{1.05-R}$ to adapt to higher loading bearing conditions.

The regression factors b and C are constant value depending on the material properties of the UGM. Korkiala-Tanttu (2009-1) has done many researches and suggest some values for b and C. Practically, C is directly dependent on the permanent deformation at the first loading step because $C * \frac{R}{1-R}$ describes the permanent deformation at the first loading step. The factor b describes how quick will be the accumulation of the permanent deformation. UGM will collapse easily and the situation is intolerable in real road construction if the b value for the UGM is larger than 0.5.

5.2 MMOPP model

MMOPP model is another model to describe the permanent deformation behaviour in UGMs. The model MMOPP (Mathematical Model of Pavement Performance) was developed by Danish researchers (Ullidtz et al 2002). The method used in MMOPP model is similar as shakedown concept. While in MMOPP model, three phases take place of three shakedown ranges.

Phase 1

Decreasing strain rate is expected in Phase 1 by plotting plastic strain versus number of loading cycles. This indicates a low stress condition. Phase 1 corresponds to shakedown Range A.

Phase 2

Constant strain rate occurs in Phase 2. The deformation behavior in Phase 2 corresponds to shakedown Range B.

Phase 3

Increasing strain rate takes place under high stress state. It is the same concept as incremental collapse (Range C).

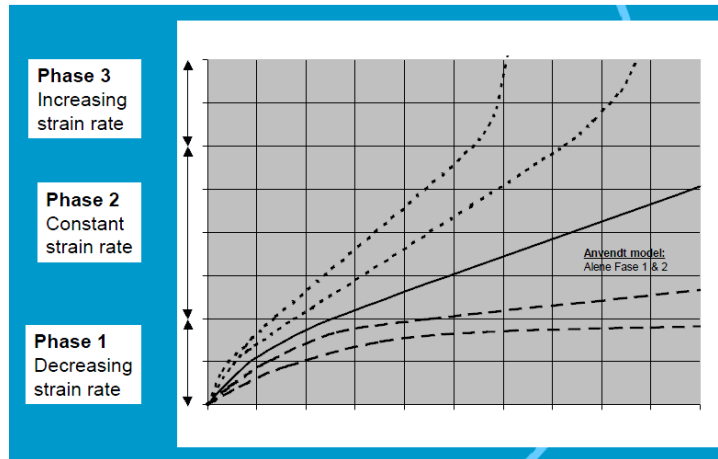


Figure 5.3 Phases described in MMOPP model (Hildebrand 2007).

The material model of MMOPP model is as follows:

$$\text{Phase 1: } \varepsilon_p = A * N^B * \left(\frac{\sigma_1}{\sigma'}\right)^C \quad (\text{for } \varepsilon_p < \varepsilon_0) \quad (\text{Eq. 5.4})$$

$$\text{Phase 2: } \varepsilon_p = \varepsilon_0 + (N - N_0) * A^{\frac{1}{B}} * B * \varepsilon_0^{1-\frac{1}{B}} * \left(\frac{\sigma_1}{\sigma'}\right)^{\frac{C}{B}} \quad (\text{for } \varepsilon_p > \varepsilon_0) \quad (\text{Eq. 5.5})$$

In which:

$$N_0 = \varepsilon_0^{\frac{1}{B}} * A^{\frac{-1}{B}} * \left(\frac{\sigma_1}{\sigma'}\right)^{\frac{-C}{B}}$$

Where:

- ε_p plastic strain
- N number of loading cycles
- σ_1 the major principal (vertical) stress
- σ' reference stress (atmospheric pressure, 0.1 Mpa)
- A, B, C model constant

In the thesis work, effort has been made to validate MMOPP model in three investigated road sections by triaxial data. However, this attempt came to an end because of the complexity of the equation and lack of literature.

5.3 Gidel model

Gidel model is another model for permanent deformation modelling of UGMs. As it has been implemented into the VägFEM program in Trafikverket, it is not collaborated here. The material model of Gidel model is as follows:

$$\epsilon_p(N) = \epsilon_1^{p0} * (1 - N)^{-B} * \left(\frac{L_{\max}}{p_a}\right)^n * \frac{1}{m + \frac{s}{p_{\max}} - \frac{q_{\max}}{p_{\max}}} \quad (\text{Eq. 5.6})$$

$$L_{\max} = \sqrt{p_{\max}^2 + q_{\max}^2}$$

Where:

ϵ_p	permanent axial strain
N	number of loading cycles
q_{\max}, p_{\max} (kPa)	maximum values of the mean principal stress p and deviatoric stress q
p_a	reference pressure (100 kPa)
ϵ_1^{p0}, B, n	model constant (regression factor in validation)
m, s	model constant, parameters of the failure line of the material

Need to mention that the denominator of Eq. 5.6 ($m + \frac{s}{p_{\max}} - \frac{q_{\max}}{p_{\max}}$), would get 0 value in the calculation. Thus when this value equals 0 or even negative value, those data should be abandoned. This would inevitably decrease the calculated permanent deformation. However, there is no other way to handle this.

6 Repeated load triaxial (RLT) test

There have been many different experimental tests which measure the deformation for pavements. For example, California Bearing Ratio (CBR) test is used to predict the behaviour of unbound granular material under static loading conditions while Falling Weight Deflectometer (FWD) tests are used to simulate the real traffic loading which provides dynamic loading conditions. Other tests like full-scale testing such as Heavy Vehicle Simulator (HVS) have very limited use because of the high expense. RLT tests are one of the most common tests for determining deformation behaviour in UGLs.

The triaxial tests are performed aiming at studying both the resilient and permanent deformation behaviour of UGMs by imposing a large number of loading repetitions on a cylindrical specimen. The loadings are imposed in form of deviatoric pressure (σ_d) and confining pressure (σ_c). According to the Swedish Standard for RLT test for unbound mixtures, there are two different types of triaxial tests depending on the manner of imposed confining pressure: the variable confining pressure method and the constant confining pressure method.

The RLT tests used in this dissertation are performed as RLT tests with constant confining pressure according to Swedish standard for cyclic load triaxial test for unbound mixtures (SVENSK STANDARD 2004).

6.1 Preparation of the specimen

Before the test, samples are taken from the in-situ pavement with sand replacement method. Specimens are prepared in a cylindrical mould where the height should be twice of the diameter ($\pm 2\%$). The specimen gets prepared in a way that five times of the diameter of the largest particle size should not exceed the diameter of the cylinder mould.

The prepared specimen is then encased by rubber membrane to prevent leakage and then placed in the triaxial apparatus. According to the European standard, the thickness of the membrane shall not exceed 0.8 percent of the diameter of the specimen. To exclude the effect of the membrane on the mechanical properties, it is required that the unstretched membrane diameter shall be no less than 95 % of the specimen diameter.

6.2 Deviatoric pressure and confining pressure

During the test, the apparatus imposes three dimensional stresses to simulate the stress state that UGMs bear under traffic loadings. The three dimensional stresses are implemented by imposing σ_d and σ_c . The deviatoric pressure σ_d is applied on the top of the specimen and the confining pressure σ_c is applied on the side of the specimen.

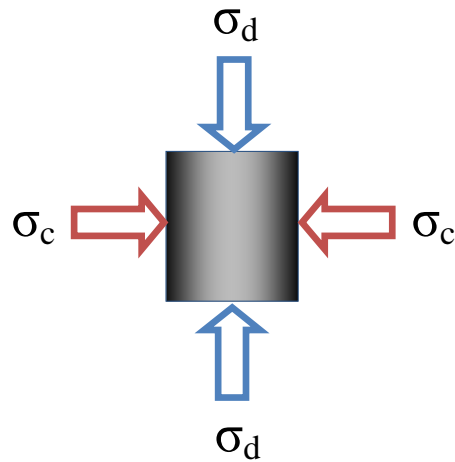


Figure 6.1 Stresses imposed on a sample in triaxial test.

In a RLT test, there are normally five or six loading sequences. In each sequence, the level of σ_c is kept constant while σ_d increases at different sequences. This is achieved by imposing a step increasing vertical deviatoric stress on top of the specimen. The confining pressure σ_c steps to a higher stress level when coming to the next sequence. In each step, σ_c is kept constant by stable water pressure surrounding the side of the specimen. The water pressure can be altered by the apparatus. In each sequence, approximately fifty thousand loading pulses are applied.

During the test, transducers in the apparatus are responsible for recording the strain responding of the specimen under three dimensional stresses. Information about the number of loading cycles, confining pressure, deviatoric pressure, elastic strain, permanent strain and so on are measured by transducers and recorded by electronic devices.

With the result of RLT tests, the shakedown range of the samples can be evaluated. Later, the factor of UGM models (both VTT and Gidel model) can be calibrated into local conditions. With calibrated factors, the rutting depth can be predicted.

7 Result

The result can be sorted in three categories:

- **Shakedown range analysis** which consists of shakedown range analysis calculated from the triaxial data. The shakedown range is calculated according to Werkmeister's theory (Eq. 3.1, Eq. 3.2 and Eq. 3.3). The shakedown range calculation is performed in the first few sequences of the triaxial test and by plotting shakedown ranges from all triaxial tests in a p–q diagram, the boundary between plastic shakedown and plastic creep can be revealed.
- **Regression factor calibration** is made by evaluating the regression factor in VTT model and Gidel model. The regression factor evaluation is made by calibrating the model prediction with the RLT tests measurement so that the model represents the real permanent deformation behaviour in the tested road.
- **Permanent deformation calculation** is performed by running FE program VägFEM loaded with VTT and Gidel model each at a time. The program covers calculation of the stress and strain state in the tested road and the permanent deformation thus can be handled with the help of that.

7.1 Shakedown range evaluation

Shakedown range evaluation has been performed on layer D1, N1, N2, N3, T1 and T3. The detailed shakedown range analysis can be found in appendix 1.

Table 7.1 Shakedown range analysis of Sample 1, Dingle.

Sequence	Number of loading cycles	Confining pressure (kPa)	Deviatoric pressure (kPa)	Shakedown range
0	10008	20	43	A
1	10008	21	62	A
2	10007	21	83	A
3	10007	21	103	A
4	10007	21	123	A
5	10008	21	143	A

Table 7.1 shows shakedown range evaluation for sample 1 from Dingle under low confining pressure. The result of shakedown range is useful in two ways. Firstly, by plotting shakedown range analysis result on p–q diagram, different shakedown limit can be defined. Secondly, Range C can be excluded from factor calibration because only Range A and Range B are valid for factor calibration in VTT and Gidel model.

Shakedown range analysis for D1, N1, N2 and T1 has been plotted in a p–q diagram.

There have been clear boundaries among different ranges, although some result collides, existing on the edges of the limits. This may due to the simplification of the way to evaluate the shakedown range (Eq. 3.1, Eq. 3.2 and Eq. 3.3) where only two points from the RLT test could decide the range of the material. However, from a larger scale, it is still feasible to find the boundaries between ranges. Two lines were drawn by hand to distinguish different ranges.

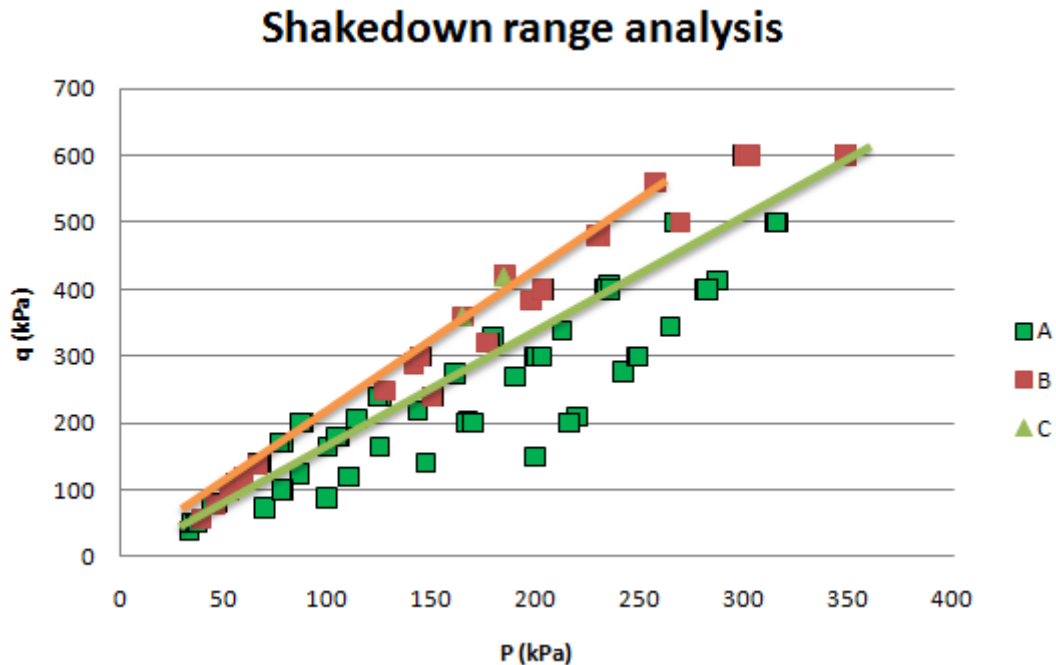


Figure 7.1 Shakedown range analyses. Green points for Range A, Red for Range B and light green for Range C. The green line represents the plastic shakedown limit and the orange line indicates the plastic creep limit.

The gradient and intercept of the limit line could be decided.

Plastic shakedown limit: $q_s = 1.64 * p + 15$ (Eq. 7.1)

Plastic creep limit: $q_c = 1.96 * p + 30$ (Eq. 7.2)

Where

q_s deviatoric stress for plastic shakedown limit (kPa)

q_c deviatoric stress for plastic creep limit (kPa)

p mean value of principal stress (kPa)

To conclude, all the values, either calculated or taken from other reports, are shown below.

Table 7.2 Shakedown limit line, creep limit line and static failure line information. (The letter “m” represents gradient of the line and “s” stands for intercept.)

Layer and location		Plastic shakedown		Plastic creep		Static failure	
		m_1	s_1	m_2	s_2	m	s
Dingle	D1	1.64	15.00	1.96	30.00	2.64	36.00
	D2	1.64	15.00	1.96	30.00	2.64	36.00
	D3	1.64	15.00	1.96	30.00	2.64	36.00
Nässjö	N1	1.64	15.00	1.96	30.00	2.64	36.00
	N2	1.64	15.00	1.96	30.00	2.64	36.00
	N3	0.77	29.00	0.88	72.00	1.72	116.00
Trädet	T1	1.64	15.00	1.96	30.00	2.64	36.00
	T2	1.64	15.00	1.96	30.00	2.64	36.00
	T3	1.31	27.75	1.53	64.63	1.87	82.00

It should be noticed that the static value of N3 and T3 are directly from Nilsson (2010). And the values of shakedown range are taken from the average value of m and s from the report (Nilsson 2010) and are filled in the table. Static values for D1, N1, N2 and T1 are from Hoff (2009).

7.2 Regression factor calibration

The regression factors for VTT model can be calculated for different location. As the RLT tests provide data about deformation, number of loading cycles, stress states and strength of the UGM which are the parameters in VTT mode, the only unknown from the model are the two regression factors: b and C. By mathematical regression analysis using the data, the factors can be solved.

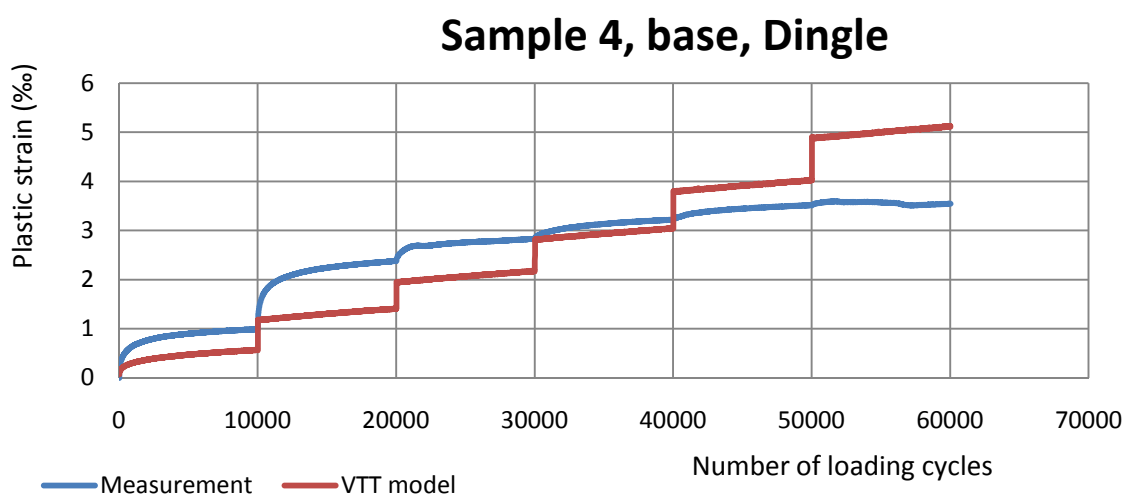


Figure 7.2 Factor calibrations for Sample 4, D1, Dingle.

As shown in the Figure 7.2, the blue curve represents the plastic strain (%) which is measured from the RLT test. The red curve is the plastic strain calculated by VTT model (Eq. 5.3). The model parameter b and C are calibrated by “solver” function in Excel program in a way that the red curve and the blue curve fit together and correlate with each other best. At last, result will predict the optimal value for b and C .

For example in the base layer of Dingle, there are four samples which are tested by RLT test and the factor is calibrated judging by all those four samples. The result based on those four samples gives b equals 0.27 and C equals 0.12. This means with these numbers as the model factor, the blue curve from VTT prediction and red curve from RLT test measurement inosculates best. Similar calibrations have been done for all tested layers (D1, N1, N2, N3, T1 and T3). The result is presented in Appendix 1. The calibrated factors are listed in table 7.3 and table 7.4.

Table 7.3 Calibrated factor for VTT model.

VTT model	Layer	C	b
Dingle	base	0.120	0.270
	subbase	0.120	0.270
	subgrade	0.120	0.270
Nässjö	base	0.038	0.218
	subbase	0.052	0.200
	subgrade	0.117	0.200
Trädet	base	0.038	0.200
	subbase	0.052	0.200
	subgrade	0.038	0.340

The calibration has limited the factor to be:

$$C \in (0.038, 0.12)$$

$$b \in (0.2, 0.4)$$

Those limits are suggested by Korkiala-Tanttu (2005). Korkiala-Tanttu has tested different material with HVS test and calculated factor C and b . She got the range for different UGMs both for in-situ condition and laboratory condition.

In the same way, Gidel model factors are calculated by correlating measured strain from RLT tests and model predicted strain. The procedure for calibration is presented in Appendix 1.

The calibrated factors are as follows.

Table 7.4 Calibrated factor for Gidel model.

Gidel model	Layer	e_{10p}	B	n
Dingle	base	4.000	0.080	0.600
	subbase	4.000	0.080	0.600
	subgrade	4.000	0.080	0.600
Nässjö	base	0.800	0.080	0.190
	subbase	2.700	0.018	1.080
	subgrade	83.429	0.001	1.832
Trädet	base	0.520	0.057	0.100
	subbase	2.700	0.018	1.080
	subgrade	53.089	0.007	0.569

The factors have been limited to:

$$e_{10p} \in \text{Free}$$

$$B \in (0, 0.1)$$

$$n \in (0, 2)$$

The factors in D1, N1, N2 and the limit for Gidel model are suggested by Hoff (2009).

7.3 Permanent deformation calculation

The permanent deformation is recalculated by the FE program VägFEM, developed by Trafikverket. With available traffic and weather condition in a specific road, the total rutting depth can be calculated. By comparing the measured rutting depth and calculated one, the prediction of the VTT model can be presented.

The FE tool “VägFEM” requires users to load data file with road information such as geometry, layer information and so forth. The data files have been done already in Trafikverket and available to use. Then parameters such as temperature distribution throughout the year (Appendix 3) and validated factors (Table 7.3 and 7.4) are required to be inputted. The button “Evaluate” will trigger the calculation of the permanent deformation.

7.3.1 Rutting calculation for Dingle and comparison

The input data for Dingle mainly remains missing. Information such as subbase, subgrade is missing. As an assumption, subbase and subgrade material are supposed to be identical as in base layer. The file for VägFEM input only includes temperature 20 °C and 30 °C without respective percentage. So it is assumed that 20 °C takes up 95 % of the annual temperature while 30 °C shares the rest 5 %.

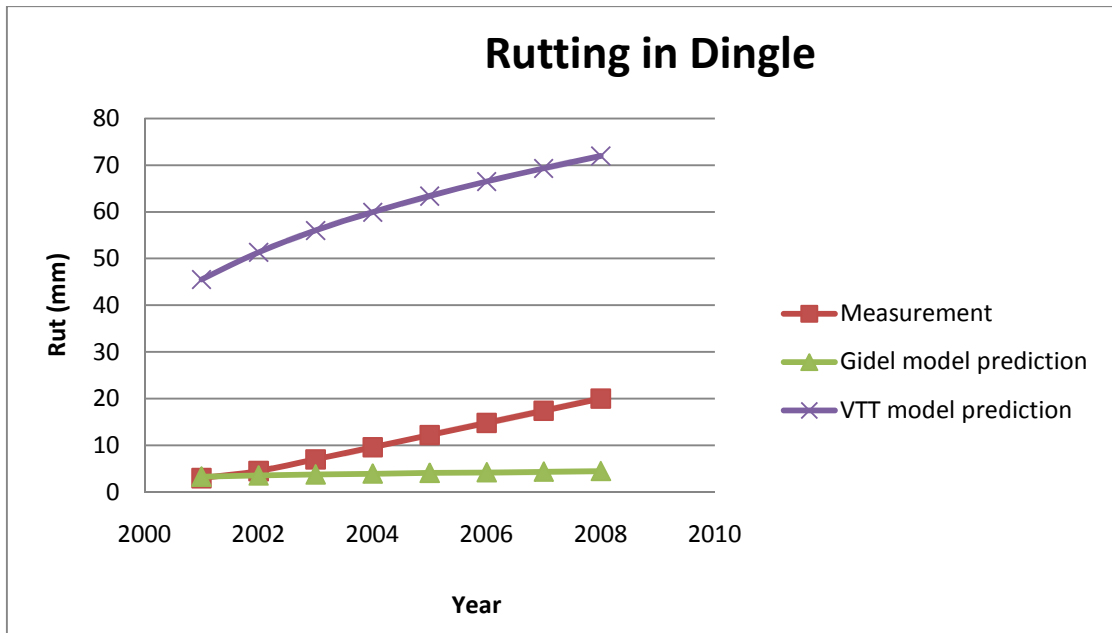


Figure 7.3 Comparisons between measured rut, VTT model prediction and Gidel model prediction for Dingle.

The result shows a high prediction from VTT model while a low prediction from Gidel model. VTT model is good at describing the shape of the rutting which is judged by the fact that the gradient of the measurement and VTT prediction curve are similar. Gidel model has closer prediction to the real rutting measurement.

7.3.2 Rutting calculation for Nässjö and comparison

In the eleven sections of road RV 31 Nässjö, road section 6 and section 11 accounts for the maximum and minimum rutting depth respectively.

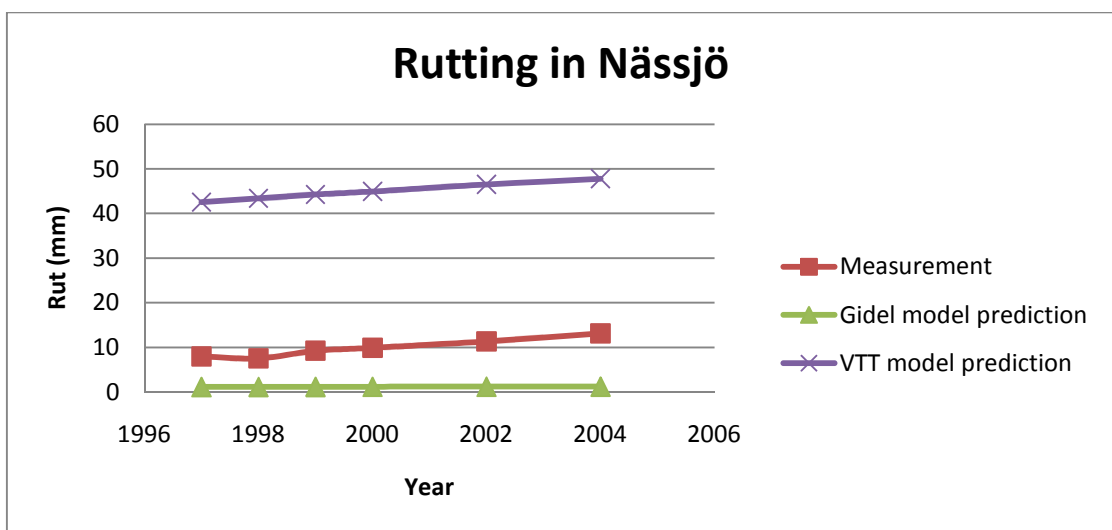


Figure 7.4 Comparisons between measured rut, VTT model prediction and Gidel model prediction for Nässjö.

The measurement value in Figure 7.4 is actually taken by the mean value of the maximum measured rutting depth and minimum measured rutting depth. Generally speaking, the prediction from Gidel model is less than measurement and VTT model have a much larger prediction.

As the measurement and prediction starts from the year 1997, when the road has almost been built for ten years, the permanent deformation is featured by a slow and steady increasing which has been correctly predicted by both models.

In the permanent deformation calculation using VTT model, the deviatoric stress q has exceeded the failure value. In another word, the failure ration R (in Eq. 5.3) is approaching to 1. This does not promise the material yielding or failure of the UGMs, because the granular materials will be bound to rotate themselves to adapt to the high stress and this movement cannot be modelled by VTT model. In VTT model, when R is exceedingly closed to 1, the shearing parameter $\frac{R}{1-R}$ will lead the plastic strain to an infinite value. This would cause overestimation on the plastic strain, which will consequently exaggerate the predicted rutting depth.

7.3.3 Rutting calculation for Trädet and comparison

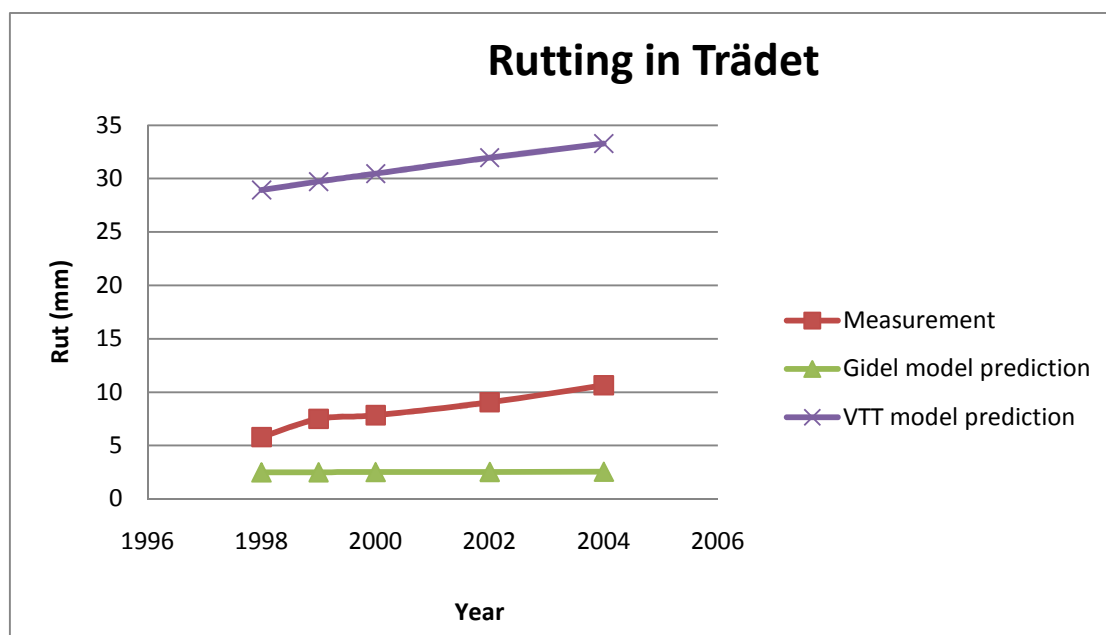


Figure 7.5 Comparisons between measured rut, VTT model prediction and Gidel model prediction for Trädet.

The prediction in Trädet predicts similar result as that from Nässjö. Gidel model has underestimated prediction while VTT model prediction is much bigger than measurement. VTT model takes advantage of accurate prediction of the increasing trend of measurement while Gidel model predict a steady and slow rutting growth.

In the permanent deformation calculation using VTT model, the R value still approached 1 after a finite loading cycles. So it is probable that the result was overestimated. As the factor $1 - R$ switches to $1.05 - R$ when q reaches the failure value, the calculated result will surely be altered in an unexpected way. For accurate

prediction, this should be avoided. This indicates that VTT model is not suitable to deal with high stress condition.

8 Sensitivity analysis

A sensitivity analysis is performed for rutting prediction model implemented with VTT model for UGLs to show how the variance in input parameters affects the output. This study will indicate which parameter is more sensitive towards the predicted rutting depth.

The method used in the sensitivity analysis is a simple linear function as follows:

$$S = \frac{\Delta F(t)/F(t)}{\Delta t/t}$$

where

S	relative value for sensitivity
$F(t)$	function where parameter t is involved
$\Delta F(t)$	increment in function
t	parameter
Δt	increment in parameter

8.1 Sensitivity analysis for rutting prediction model implemented with VTT model

The rutting prediction model integrates models for asphalt layers and UGLs. In this study, only rutting prediction model implemented with VTT model is analysed. The calculated rutting depth $F(N, b, C, m, s \dots)$ is a function of several parameters such as number of loading cycles (N), VTT model factors (b and C), material failure properties (m and s). Sensitivity analysis is performed for all these parameters by increasing them by 1 % as the increment. The analysis is done only for Nässjö and it is believed that the result from Nässjö will be representative.

8.2 Result

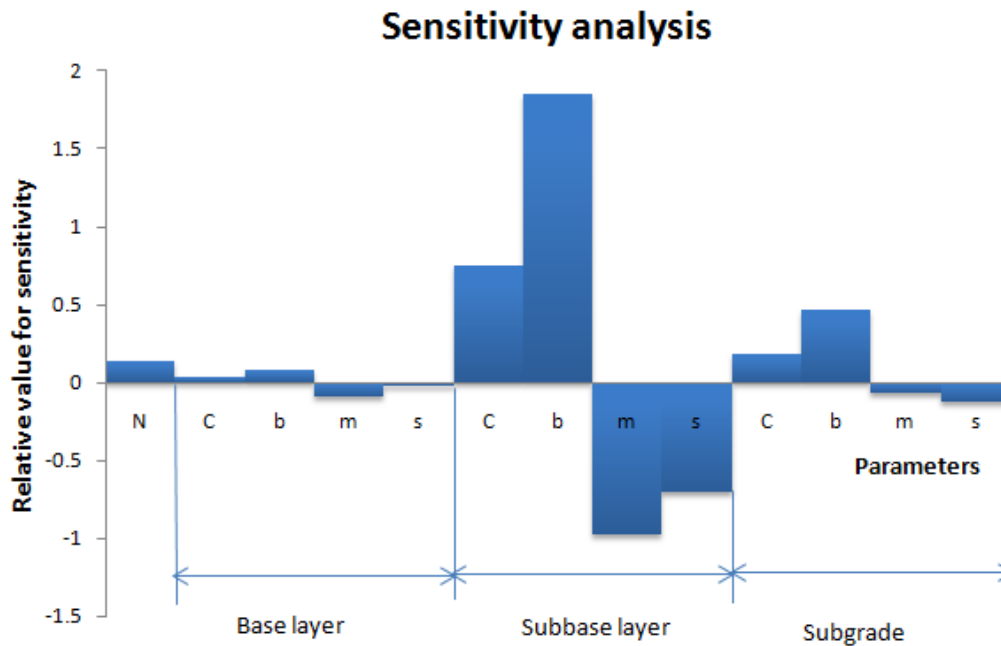


Figure 8.1 Sensitivity analysis.

The result has shown that the parameters from the subbase layer acts as the most sensitive layer as the relative value for sensitivity is always larger compared with other layers. Thus the material in subbase layer should have better quality in order to resist rutting in the pavement.

The VTT model factor b is the most sensitive parameters for each layer which mean that the risk of error in factor b will dominate the error in the result. To minimize error in predicted rutting, the most sensitive parameters are always required to be more accurate. Among all factors, it is noticeable that the factor b from subbase layer is the most sensitive parameter.

It is worthy mentioning that the material failure parameter (m and s) presents negative value for sensitivity. This means when these parameters increase, the predicted rutting depth will decrease. This happens in real situation because that the increase of m and s promising better resistance towards shearing damage and will help to reduce permanent deformation. So it would be a priority to use better UGMs for resisting rutting while limiting heavy vehicle volume comes after.

9 Discussion

The comparison of permanent deformation by VTT model, Gidel model and rutting measurement shows that VTT model overestimates the rutting depth and Gidel model underestimates the rutting depth. The advantage of VTT model is that it could predict the development of rutting which is demonstrated by similar shape of the curves (judging by Figure 7.3, 7.4 and 7.5). The prediction from Gidel model is a little less than measurement but not as much as the amount of overestimation by VTT model.

VTT model predicts the development of rutting although overestimates it which means large error in the prediction. This means VTT model is precise but not accurate enough. The most probable reason should be the defect of the model that it could not be applied for high stress condition which is also the defect for all other UGM models. Another reason could be the system error caused by assumptions. This could be fixed by adjusting the model.

Sensitivity study shows that the most sensitive parameter of VTT model is the factor b . So it is really important to validate the model with accurate factors. Despite of its high expense, HVS is the best test to validate the model as the author of VTT model suggested. Triaxial test is applicable but it is not the first choice as long as financing is not a problem.

As indicated in sensitivity analysis, the static test result which reflects the material failure properties is also of importance. The static failure line, if possible, should be plotted for each sample, rather than make one failure line for different samples because they have different resistance towards failure.

There is also a hint that all parameters from the subbase layer are more sensitive than the same parameter from other UGLs. This means the material in the subbase layer is very critical in predicting permanent deformation. So for construction, better materials should be used in subbase to help resist rutting.

10 Conclusion and recommendation

Judging by the comparison, there is clear evidence that VTT model is capable of predicting rutting in three investigated roads, while the prediction is overestimated because of high stress in the pavement. The model takes consideration of the shearing property which simply can show the stress level by a single parameter R, although the prediction could be exaggerated by that. A few recommendations are proposed for better application of VTT model:

- The prediction from VTT model is very good at describing the gradient of rutting curve graphically which is to say VTT model is capable of predicting the development of rutting, although the prediction overestimates the rutting measurement.
- Better prediction can be made by VTT model within pavement under low stress level. High stress level can cause overestimation in predicted rutting depth. This could also be a hint that during pavement construction, it is important to avoid high stress to help accurate predicting of rutting depth.
- In the view of rutting prediction, it is very important to get the accurate factors for getting better prediction. Because the factor will have great impact on the result. It is recommended using HVS test to simulate the real pavement structure under repeated loading. RLT test reflects the material properties however it is affected by many other factors such as sample conditions, which might bias the real material response.
- In the view of construction, to use better material with higher failure resistance capacity is favorable in reducing rutting. Limiting the volume of heavy vehicle is just a second option.
- The result of static failure test is also of importance. The sensitivity of failure parameters m and s are the second most sensitive parameters besides factors b and C from VTT model. Thus it would be much better to plot static failure line for each sample in order to predict rutting more accurately.
- More investigation should be done in the layer where the material properties are unknown (D2, D3 and T2) to avoid errors in the result. Too many assumptions will bring about larger uncertainties into the model.

It is need to declare that one important assumption for the validation is the equivalence of the number of loading cycles from RTL test (N) and the cumulative ESAL. They must be relevant to each other but are not the same concept. Further study should be performed to arrive in a successful conversion between N and cumulative ESAL. Another way to implement the conversion is by adding a reduction factor to the result which means to modify the total permanent deformation by a certain proportion.

11 References

- Dawson et al. (1999): Dawson A R, Wellner F, Plastic Behaviour of Granular Materials. Department of Civil Engineering, University of Nottingham, 1999.
- Ekblad (2004): Ekblad J, Influence of water on resilient properties of coarse granular materials, Royal Institute of Technology (KTH), Stockholm, Sweden.
- Hildebrand 2007: Hildebrand G, Performance Prediction Models in MMOPP, Danish Road Directorate, 2007.
- Hoff (1999-1): Hoff I, Constitutive Model for Unbound Granular Materials Based on Hyperelasticity, 1999.
- Hoff (1999-2): Hoff I, Material properties of unbound aggregates for pavement structures, PhD thesis, Technical University of Norway (NTNU), Trondheim, Norway.
- Hoff (2009): Hoff I, Triaxial test result, Performance Prediction Models for Flexible Pavements Part 2; Project Level, 2009. Trondheim, Norway.
- Huang (2004): Huang Y H, Pavement Analysis and Design (Pearson Education, Inc. Upper Saddle River, NJ 07458, Second edition). pp. 9-10.
- Huvstig (2009): Huvstig A, Performance Prediction Models for Flexible Pavements Part 2; Project Level, Description of test sites. Trafikverket, Gothenburg, Sweden.
- Korkiala-Tanttu (2005): Ny Media AS: A new material model for permanent deformations in pavements, In: Proc. of the Seventh Conference on Bearing Capacity of Roads and Airfields, Trondheim, 2005.
- Korkiala-Tanttu (2009-1): Korkiala-Tanttu L, Calculation Method for Permanent Deformation of Unbound Pavement Materials, Doctoral dissertation. Department of Civil and environmental Engineering, Helsinki University of Technology, 2009.
- Korkiala-Tanttu (2009-2): Korkiala-Tanttu L, Calculation Method for Permanent Deformation of Unbound Pavement Materials, Doctoral dissertation. Department of Civil and environmental Engineering, Helsinki University of Technology, pp 37, 2009.
- NCHRP (2004): Mechanistic-Empirical design of new & rehabilitated pavement structures. American Association of State Highway and Transportation Officials (AASHTO), Washington DC, USA.
- Nilsson (2010): Triaxialförsök, Bestämning av motståndskraft mot permanenta deformationer hos befintligt terrassmaterial, Skanska Sverige AB, 2010.
- PCA 2010: Waikiki Says "Aloha" to Integrated Paving Systems Approach (http://www.cement.org/pavements/pv_int_kalia.asp), Portland Cement Association, 2010.
- SVENSK STANDARD 2004: Unbound and hydraulically bound mixtures - Part 7: Cyclic load triaxial test for unbound mixtures, English version, SVENSK STANDARD SS-EN 13286-7: 2004, European standard, EN 13286-7: 2004, European Committee for Standardization, 2004.
- Ullidtz et al 2002: Ullidtz P, Analytical tools for design of flexible pavements, proceeding of the International Conference on Asphalt Pavements, Denmark, 2002.

Werkmeister (2003-1): Werkmeister S, Permanent Deformation Behaviour of Unbound Granular Materials in Pavement Constructions, Dissertation. Dresden University of Technology, Germany, pp 4-2, 2003.

Werkmeister (2003-2): Werkmeister S, Permanent Deformation Behaviour of Unbound Granular Materials in Pavement Constructions, Dissertation. Dresden University of Technology, Germany, pp 4-2, 4-7, 2003.

Werkmeister (2003-3): Werkmeister S, Permanent Deformation Behaviour of Unbound Granular Materials in Pavement Constructions, Dissertation. Dresden University of Technology, Germany, pp 6-7, 2003.

Werkmeister (2003-4): Werkmeister S, Permanent Deformation Behaviour of Unbound Granular Materials in Pavement Constructions, Dissertation. Dresden University of Technology, Germany, pp 5-5, 5-6, 2003.

12 Appendix

Appendix 1.....	40
Appendix 2.....	65
Appendix 3.....	68
Appendix 4.....	69
LIST OF FIGURES	72
LIST OF TABLES	74

12.1 Appendix 1

Location Dingle

Layer Base layer

Data

Sample 1 = Dingle1

Sample 2 = Dingle2Elas

Sample 3 = Dingle3

Sample 4 = Dingle4

RTL tests

Sample 1

Table 13.1 Shakedown range evaluation result for sample 1, base, Dingle.

Sequence	Number of loading cycles	Confining pressure (kPa)	Deviatoric pressure (kPa)	Shakedown range
0	10008	20	43	A
1	10008	21	62	A
2	10007	21	83	A
3	10007	21	103	A
4	10007	21	123	A
5	10008	21	143	A

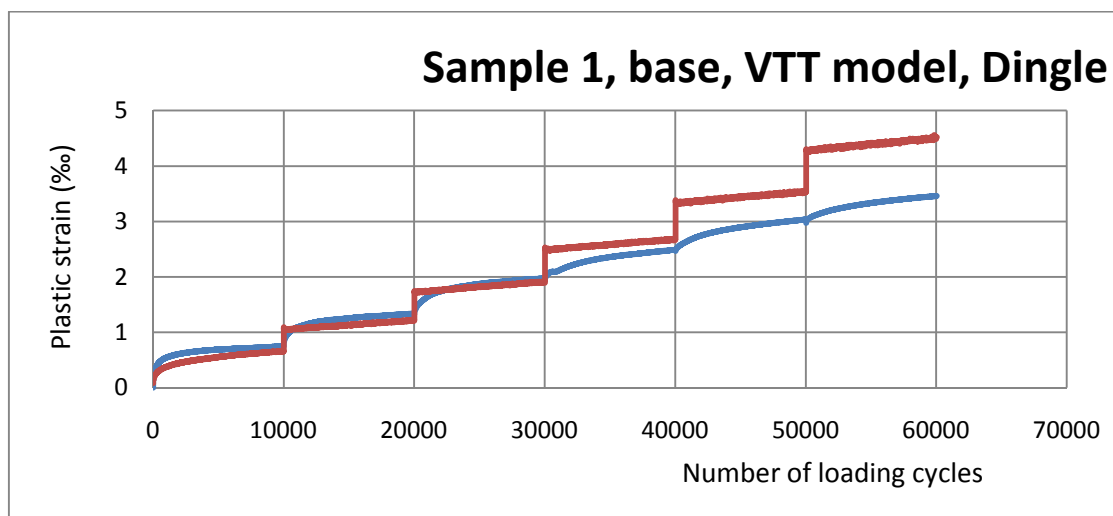


Figure 13.1 VTT model factors calibrations with RL data, sample 1, Base, Dingle.

Sample 2

Sample 2 is not taken into validation because the loading step is not plentiful (413 loading cycles in total).

Sample 3

Table 13.2 Shakedown range evaluation result for sample 3, base, Dingle.

Sequence	Number of loading cycles	Confining pressure (kPa)	Deviatoric pressure (kPa)	Shakedown range
0	10004	45	79	A
1	10005	45	141	B
2	10010	46	184	B
3	10002	46	226	B
4	2247	46	268	-

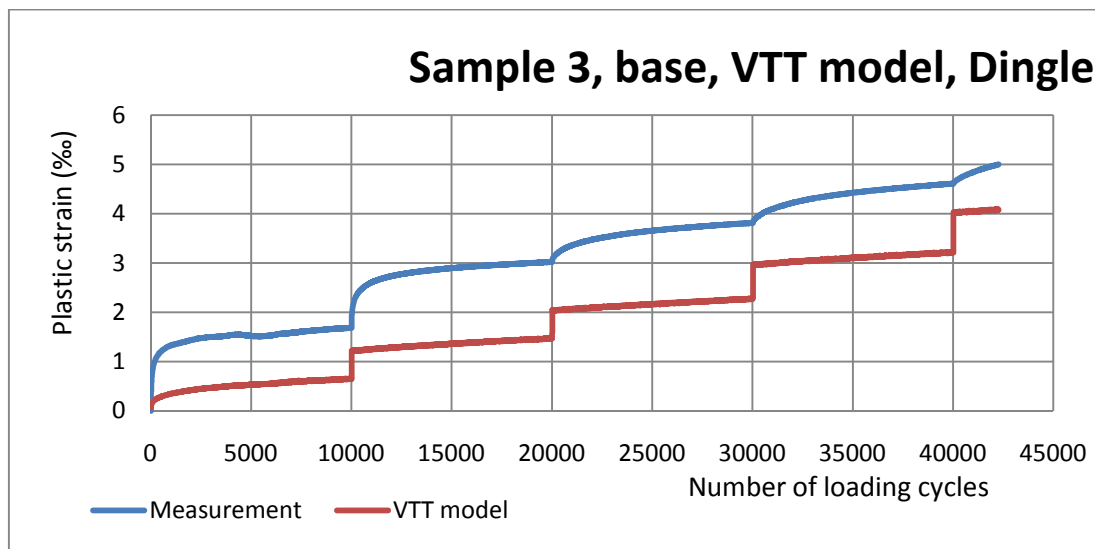


Figure 13.2 VTT model factors calibrations with RLT data, sample 3, Base, Dingle.

Sample 4

Table 13.3 Shakedown range evaluation result for sample 4, base, Dingle.

Sequence	Number of loading cycles	Confining pressure (kPa)	Deviatoric pressure (kPa)	Shakedown range
0	10006	70	98	B
1	10008	70	183	B
2	10003	70	239	A
3	10005	70	296	B
4	10006	70	351	A
5	10006	70	407	A

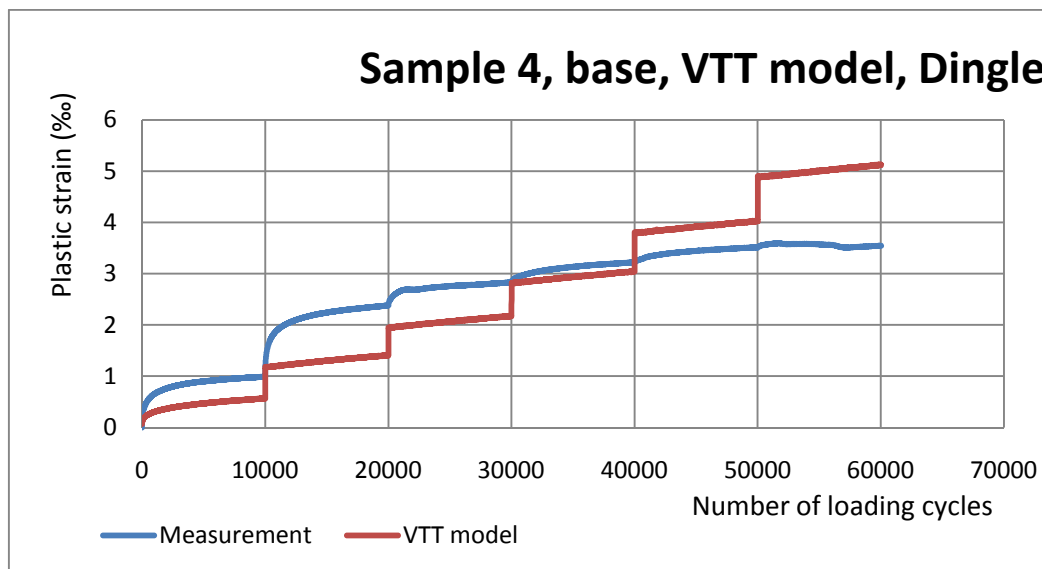


Figure 13.3 VTT model factors calibrations with RLT data, sample 4, Base, Dingle.

Location Nässjö
Layer Base layer

Data

Sample 1 = Na1FM10C
 Sample 2 = Na2FM20
 Sample 3 =Na3FM40
 Sample 4 =Na4FM40
 Sample 5 =Na5FM80

RTL tests

Sample 1

Table 13.4 Shakedown range evaluation result for sample 1, base, Nässjö.

Sequence	Number of loading cycles	Confining pressure (kPa)	Deviatoric pressure (kPa)	Shakedown range
0	10003	18	50	A
1	10008	18	80	A
2	10008	19	110	A
3	10004	21	140	A
4	10005	21	170	A
5	10007	21	200	A

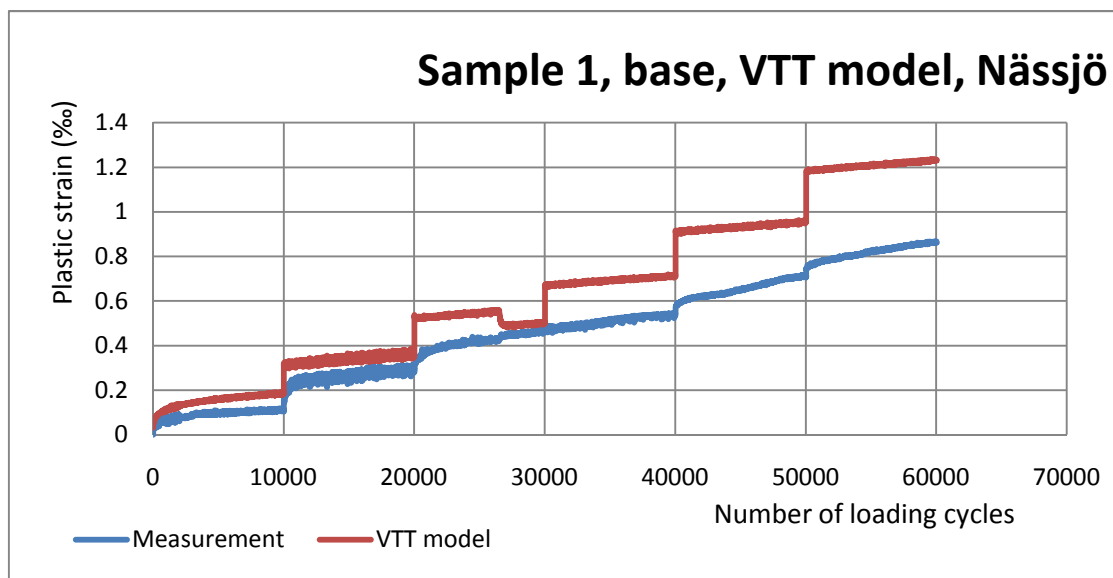


Figure 13.4 VTT model factors calibrations with RLT data, sample 1, Base, Nässjö.

Sample 2

Table 13.5 Shakedown range evaluation result for sample 2, base, Nässjö.

Sequence	Number of loading cycles	Confining pressure (kPa)	Deviatoric pressure (kPa)	Shakedown range
0	10006	20	50	A
1	10010	20	80	A
2	10003	20	110	A
3	10005	20	140	A
4	10009	20	170	A
5	10003	20	200	A

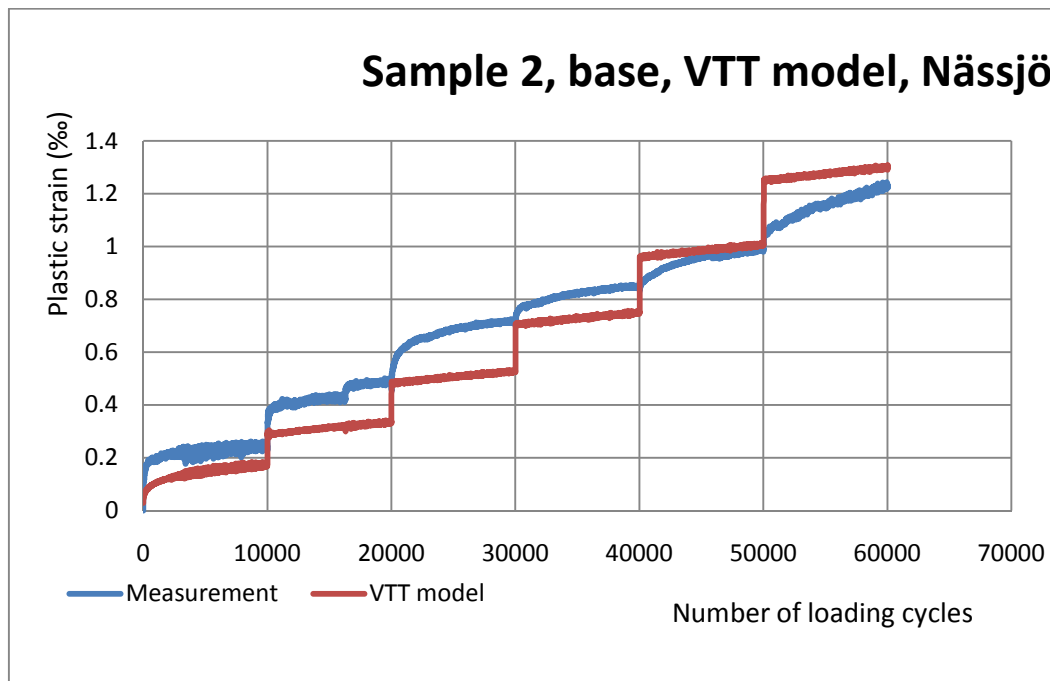


Figure 13.5 VTT model factors calibrations with RLT data, sample 2, base, Nässjö.

Sample 3

Table 13.6 Shakedown range evaluation result for sample 3, base, Nässjö.

Sequence	Number of loading cycles	Confining pressure (kPa)	Deviatoric pressure (kPa)	Shakedown range
0	10003	16	50	A
1	10004	16	80	B
2	10009	16	110	B
3	10004	16	140	B
4	10007	16	170	A
5	10003	16	200	B

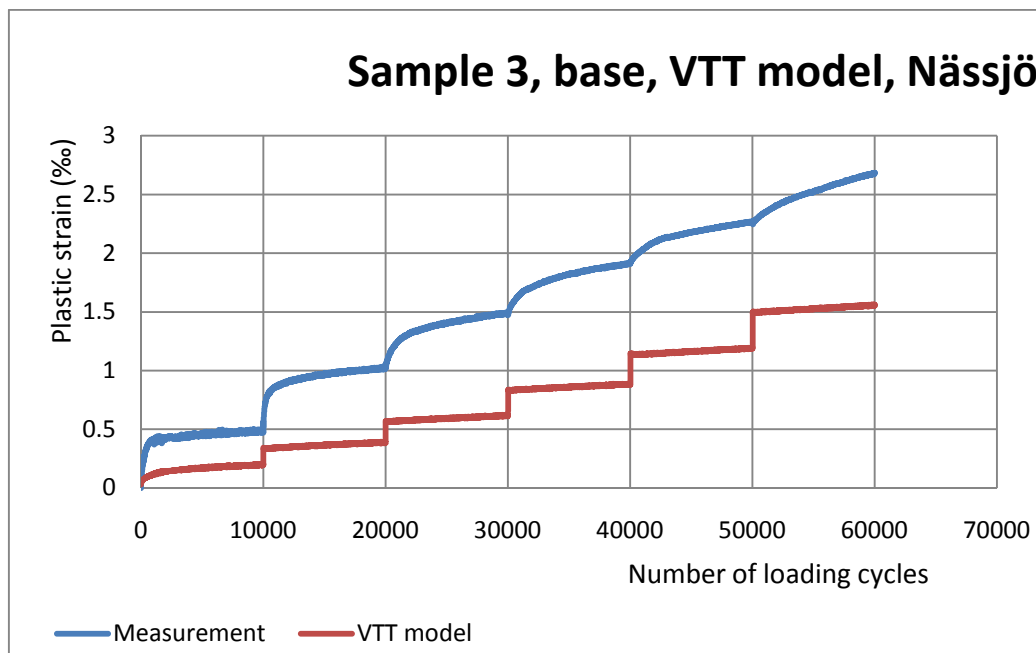


Figure 13.6 VTT model factors calibrations with RLT data, sample 3, base, Nässjö.

Sample 4

Table 13.7 Shakedown range evaluation result for sample 4, base, Nässjö.

Sequence	Number of loading cycles	Confining pressure (kPa)	Deviatoric pressure (kPa)	Shakedown range
0	10006	45	100	A
1	10005	45	180	A
2	10009	45	240	A
3	10007	45	300	B
4	10006	45	360	B
5	9994	45	420	B

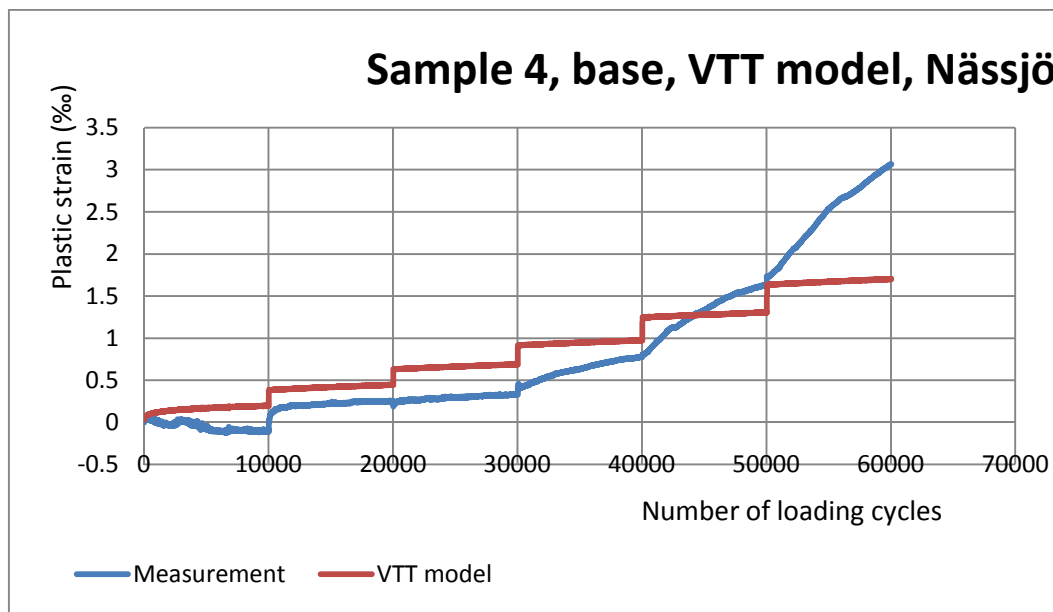


Figure 13.7 VTT model factors calibrations with RLT data, sample 4, base, Nässjö.

Sample 5

Table 13.8 Shakedown range evaluation result for sample 5, base, Nässjö.

Sequence	Number of loading cycles	Confining pressure (kPa)	Deviatoric pressure (kPa)	Shakedown range
0	10007	70	120	A
1	10007	70	240	A
2	10006	69	320	A
3	10007	70	400	A
4	10007	70	480	A
5	10014	70	560	A

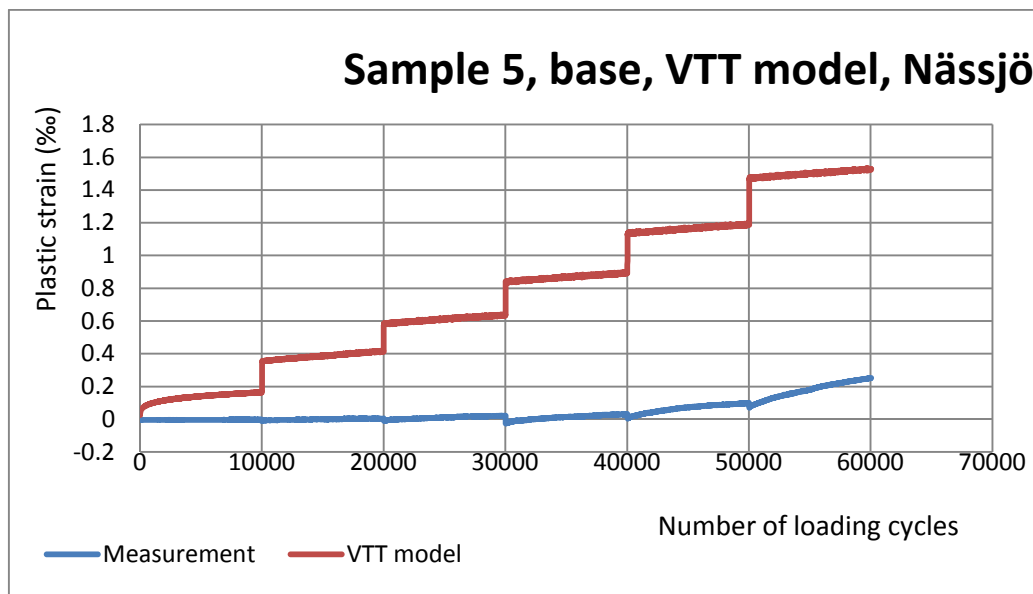


Figure 13.8 VTT model factors calibrations with RLT data, sample 5, base, Nässjö.

Location Nässjö
Layer Subbase layer

Data

Sample 1 = NaF1FM10 (version 2)

Sample 2 =NaF2FM20 cond

Sample 3 =NaF3FM40

Sample 4 =NaF4FM80

RLT tests result

Sample 1

Table 13.9 Shakedown range evaluation result for sample 1, subbase, Nässjö.

Sequence	Number of loading cycles	Confining pressure (kPa)	Deviatoric pressure (kPa)	Shakedown range
0	10006	20	50	A
1	10009	20	80	A
2	10010	20	110	A
3	10003	20	140	A
4	10007	20	170	A
5	10011	20	200	A

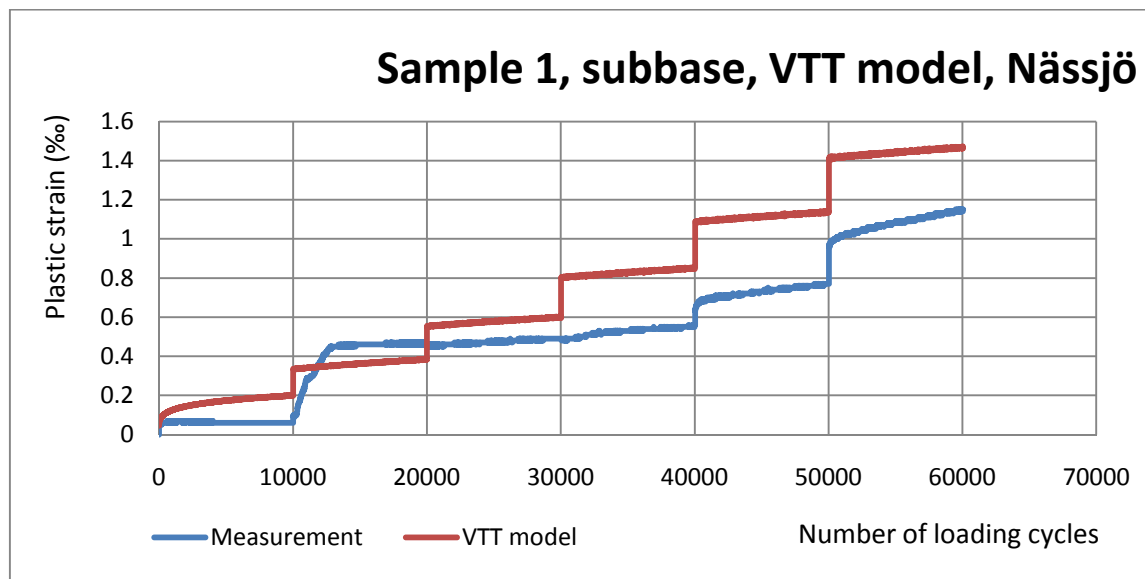


Figure 13.9 VTT model factors calibrations with RLT data, sample 1, subbase, Nässjö.

Sample 2

Table 13.10 Shakedown range evaluation result for sample 2, subbase, Nässjö.

Sequence	Number of loading cycles	Confining pressure (kPa)	Deviatoric pressure (kPa)	Shakedown range
0	20007	70	340	B

The total number of loading cycles is 20007 which is as twice much as a normal sequence. However sample 2 is still considered in the validation to show the effect of higher confining pressure which is approximately 70 kPa.

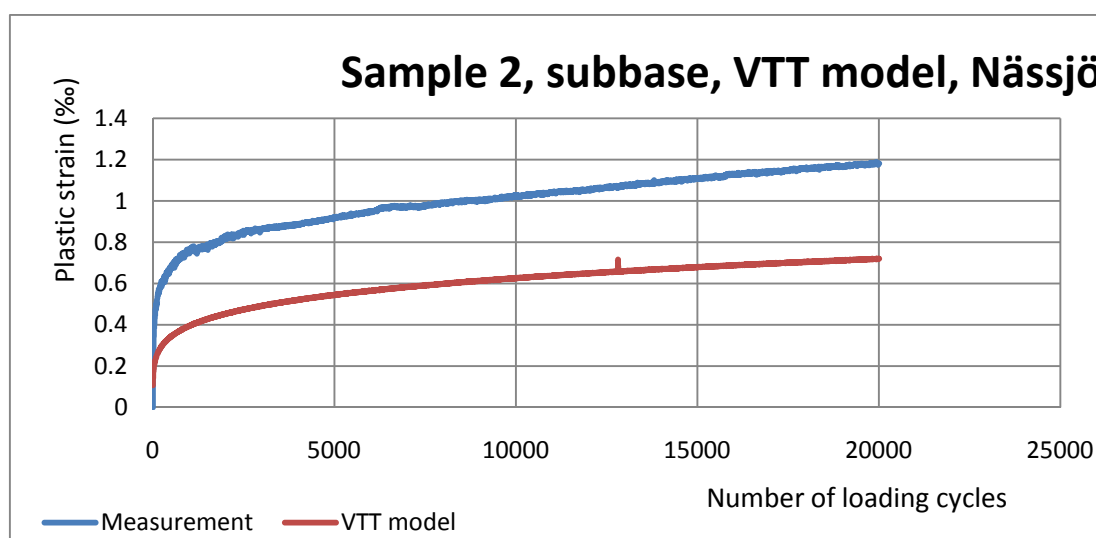


Figure 13.10 VTT model factors calibrations with RLT data, sample 2, subbase, Nässjö.

Sample 3

Table 13.11 Shakedown range evaluation result for sample 3, subbase, Nässjö.

Sequence	Number of loading cycles	Confining pressure (kPa)	Deviatoric pressure (kPa)	Shakedown range
0	10006	44	100	A
1	10006	44	180	A
2	10009	44	240	B
3	10008	44	300	A
4	10009	44	360	C
5	698	44	419	-

Sequence 0 is excluded in calibration for factors of VTT model because there is a sudden drop in the measured permanent strain. Similarly, sequence 3 is excluded as well. Sequence 4 and 5 are also excluded because the model can be only applied for shakedown range A and B.

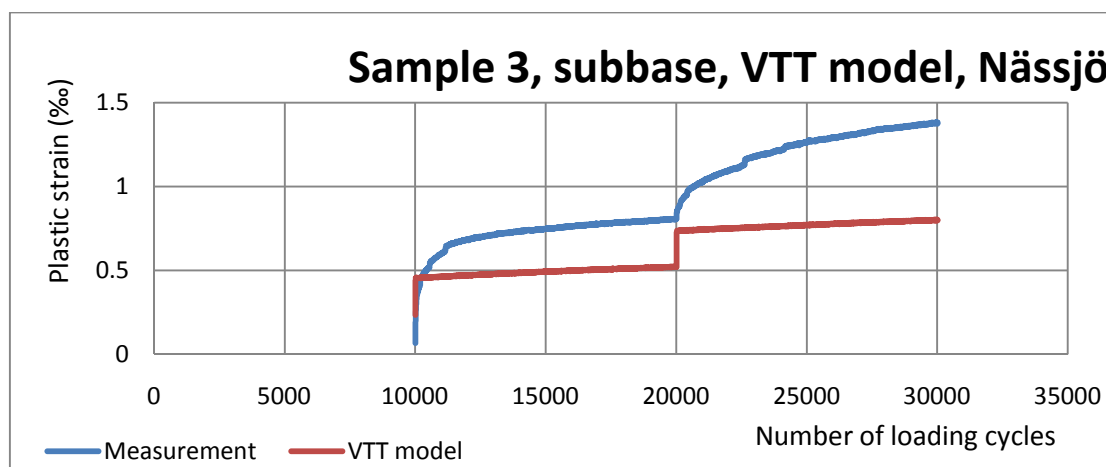


Figure 13.11 VTT model factors calibrations with RLT data, sample 3, subbase, Nässjö.

Sample 4

Table 13.12 Shakedown range evaluation result for sample 4, subbase, Nässjö.

Sequence	Number of loading cycles	Confining pressure (kPa)	Deviatoric pressure (kPa)	Shakedown range
0	10006	20	50	A
1	10008	20	80	A
2	10005	20	110	A
3	10007	20	140	A
4	10002	20	170	A
5	10011	20	200	A

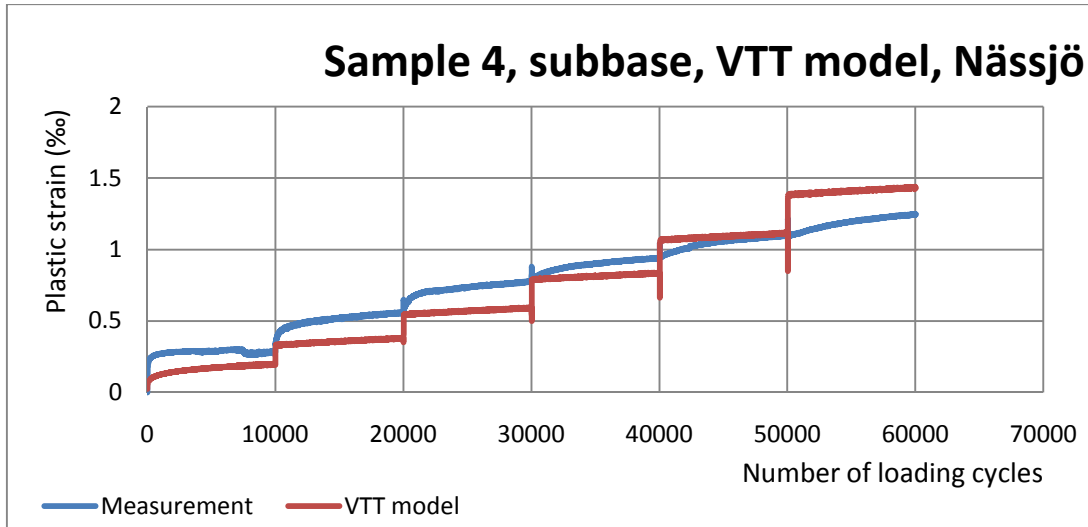


Figure 13.12 VTT model factors calibrations with RLT data, sample 4, subbase, Nässjö.

Location Nässjö
Layer Subgrade

Data

Sample 1 = 61

Sample 2 = 62

Sample 3 = 63

Sample 4 = 64

RLT tests

Triaxial data for subgrade, Nässjö includes four tests. The samples are tested under different level of confining pressure. For validation, only the data from the first few sequences with initial confining pressure is used.

Sample 1

Table 13.13 Shakedown range evaluation result for sample 1, subgrade, Nässjö.

Sequence	Number of loading cycles	Confining pressure(kPa)	Deviatoric pressure (kPa)	Shakedown range
0	10000	15	15	A
1	427	15	30	-

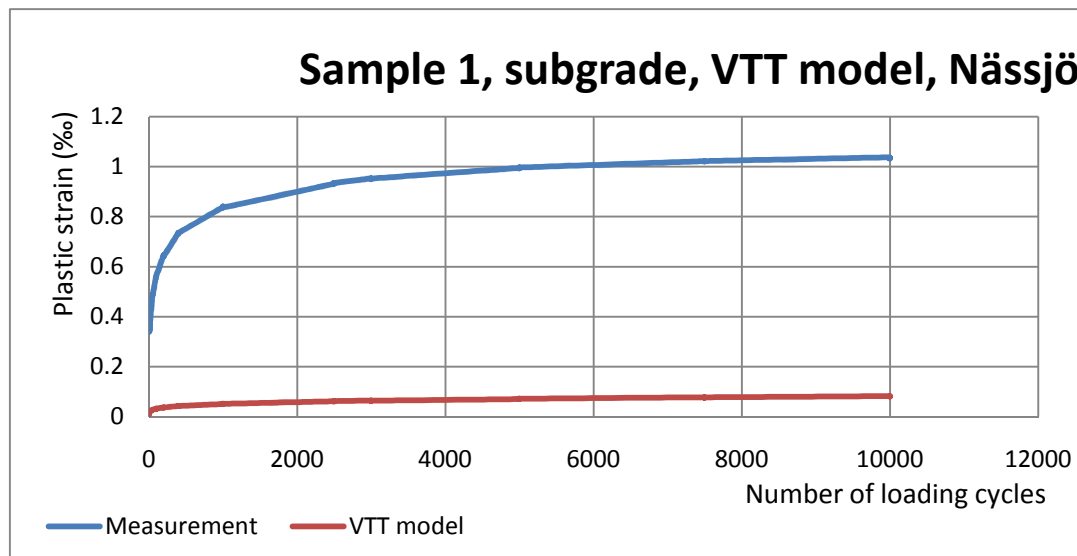


Figure 13.13 VTT model factors calibrations with RLT data, sample 1, subgrade, Nässjö.

The shakedown limit from sequence 1 is unknown because of the limited loading cycles. Thus only sequence 0 is considered in the factor calibration.

Sample 2

Table 13.14 Shakedown range evaluation result for sample 2, subgrade, Nässjö.

Sequence	Number of loading cycles	Confining pressure (kPa)	Deviatoric pressure (kPa)	Shakedown range
0	10000	20	50	A
1	10000	20	80	A
2	10000	20	110	B
3	10000	20	140	B
4	10000	20 <td 170	B	
5	10000	20	200	C

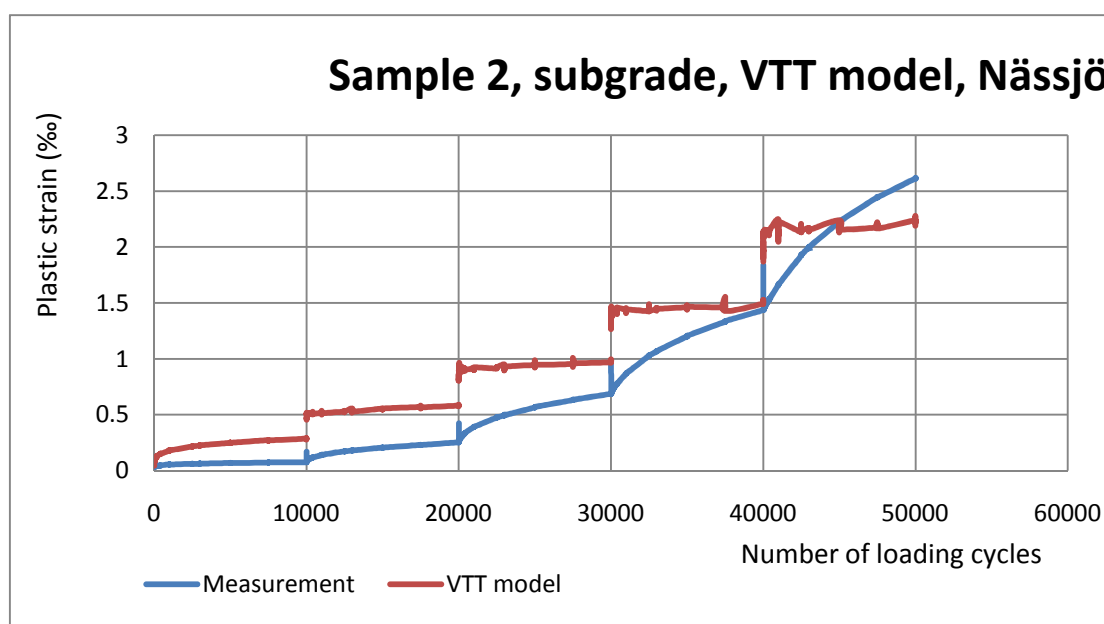


Figure 13.14 VTT model factors calibrations with RLT data, sample 2, subgrade, Nässjö.

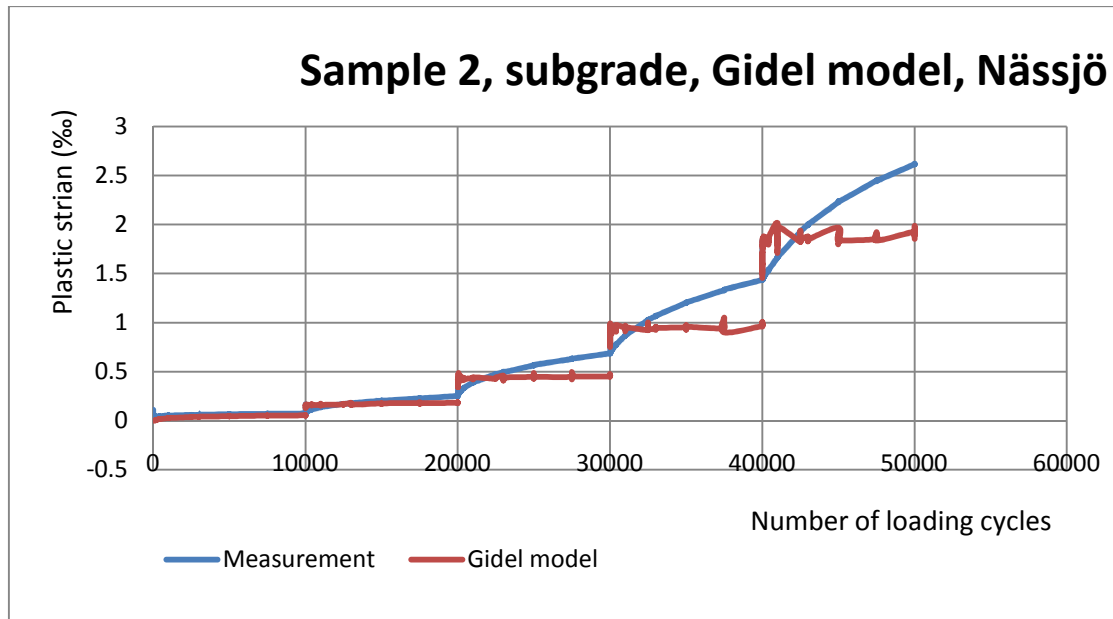


Figure 13.15 Gidel model factors calibrations with RLT data, sample 2, subgrade, Nässjö.

Sample 3

Table 13.15 Shakedown range evaluation result for sample 3, subgrade, Nässjö.

Sequence	Number of loading cycles	Confining pressure (kPa)	Deviatoric pressure (kPa)	Shakedown range
0	10000	20	20	A
1	10000	20	40	B
2	10000	20	60	B
3	578	20	80	-

Only sequence 0, 1, 2 are taken into consideration in the factor calibration.

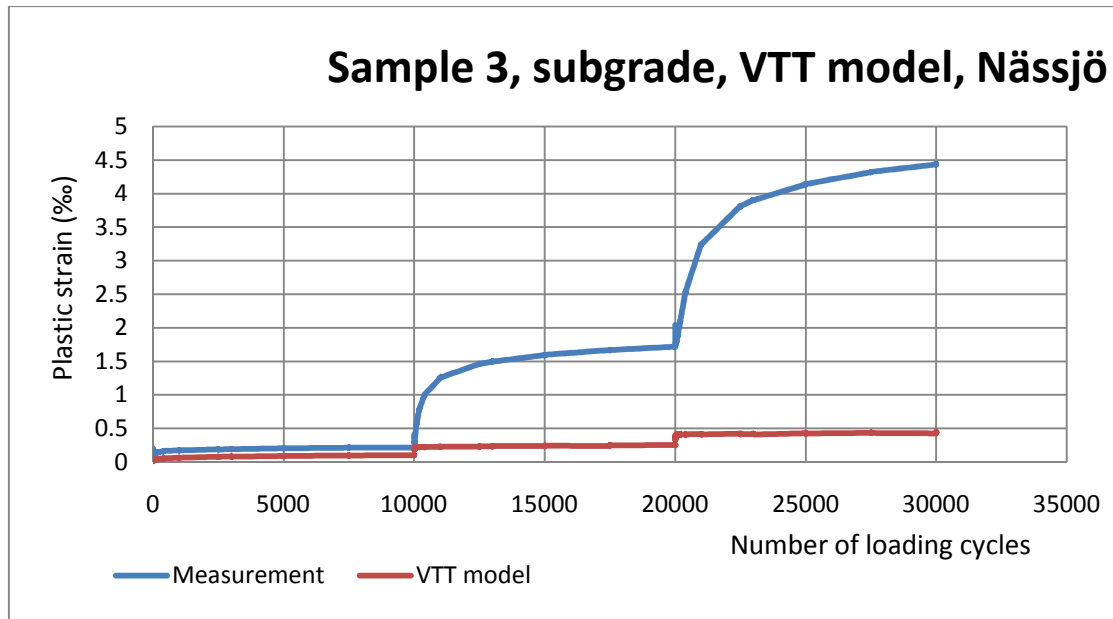


Figure 13.16 VTT model factors calibrations with RLT data, sample 3, subgrade, Nässjö.

Sample 4

Table 13.16 Shakedown range evaluation result for sample 4, subgrade, Nässjö.

Sequence	Number of loading cycles	Confining pressure (kPa)	Deviatoric pressure (kPa)	Shakedown range
0	10000	20	50	A
1	10000	20	80	B
2	10000	20	110	B
3	3620	20	140	-

Sequence 3 is excluded in the factor calibration.

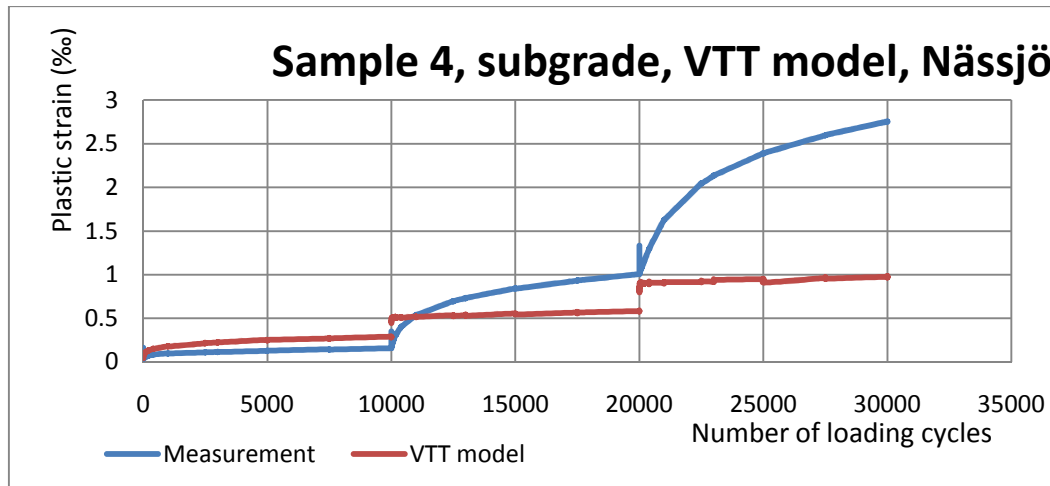


Figure 13.17 VTT model factors calibrations with RLT data, sample 4, subgrade, Nässjö.

For the validation of Gidel model, the first validation is based on data from all four triaxial tests, however, unreasonable values are obtained ($n = 0$). Thus only sample 2 is selected for validating.

Location Trädet

Layer Base layer

RLT tests result

Sample 1

Table 13.17 Shakedown range evaluation result for sample 1, base, Trädet.

Sequence	Number of loading cycles	Confining pressure (kPa)	Deviatoric pressure (kPa)	Shakedown range
0	10003	20	50	A
1	10007	20	80	A
2	10004	20	110	A
3	10011	20	140	A
4	10005	20	170	A
5	10004	20	200	A

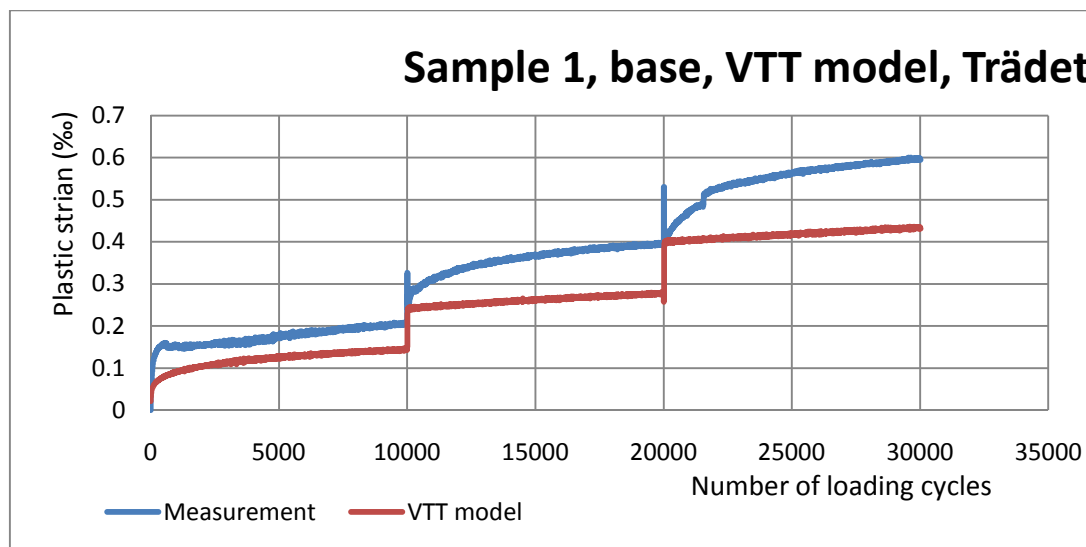


Figure 13.18 VTT model factors calibrations with RLT data, sample 1, base, Trädet.

Sample 2

Table 13.18 Shakedown range evaluation result for sample 2, base, Trädet.

Sequence	Number of loading cycles	Confining pressure (kPa)	Deviatoric pressure (kPa)	Shakedown range
0	10002	46	100	A
1	10006	45	180	A
2	10009	45	240	A
3	10003	45	300	A
4	10011	45	360	A
5	10010	45	420	A

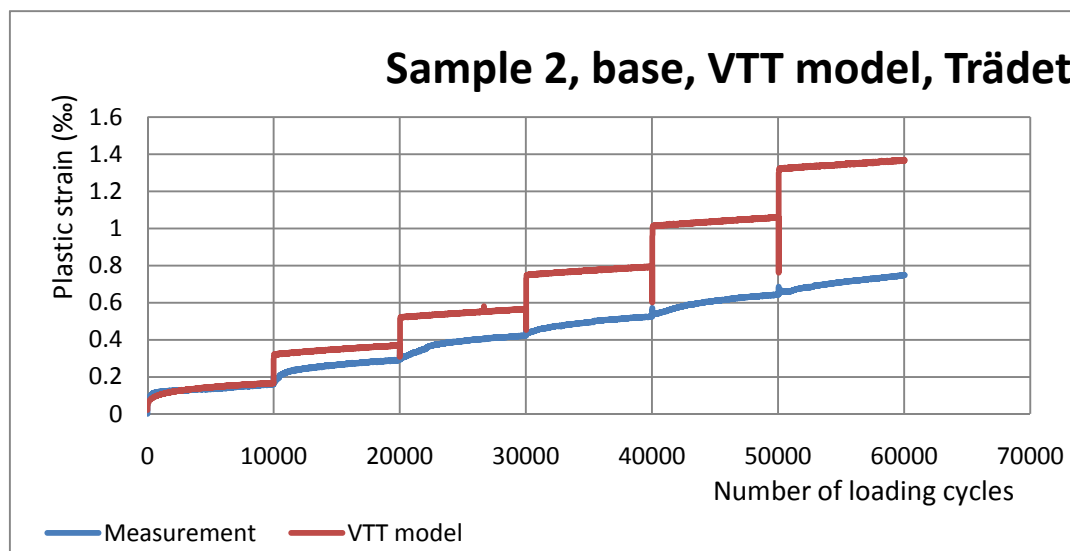


Figure 13.19 VTT model factors calibrations with RLT data, sample 2, base, Trädet.

Sample 3

Sample 3 has been neglected because of the plentiful negative data in permanent strain which is not a usual situation.

Location Trädet

Layer Subgrade

Data

Sample 1 = 51

Sample 2 = 52

Sample 3 = 53

Sample 4 = 54

RLT tests result

Sample 1

Table 13.19 Shakedown range evaluation result for sample 1, subgrade, Trädet.

Sequence	Number of loading cycles	Confining pressure (kPa)	Deviatoric pressure (kPa)	Shakedown range
0	10000	20	50	A
1	10000	20	80	A
2	10000	20	110	A
3	10000	20	140	A
4	422	20	170	-

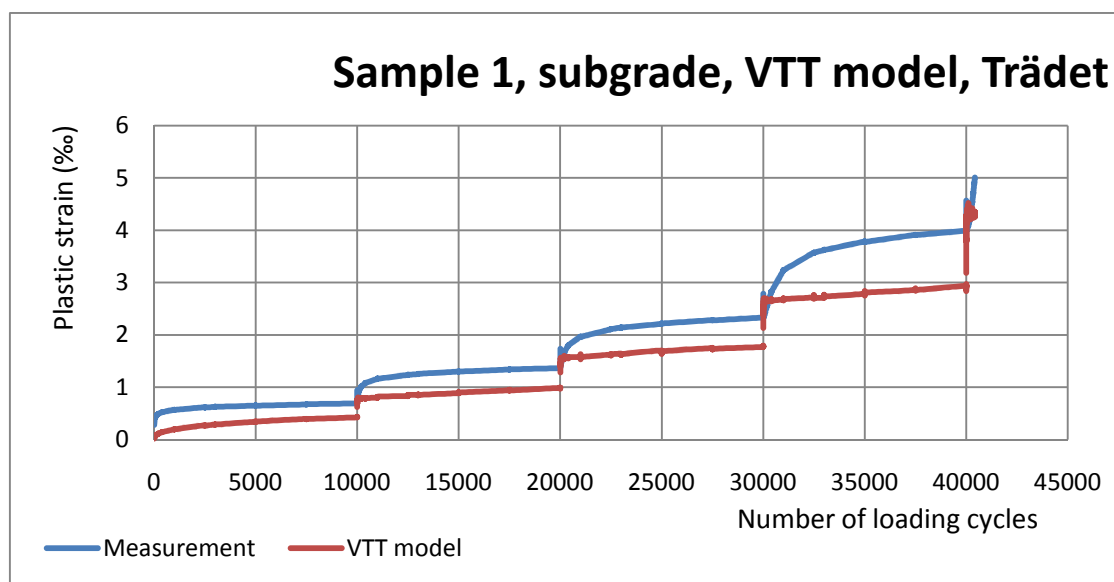


Figure 13.20 VTT model factors calibrations with RLT data, sample 1, subgrade, Trädet.

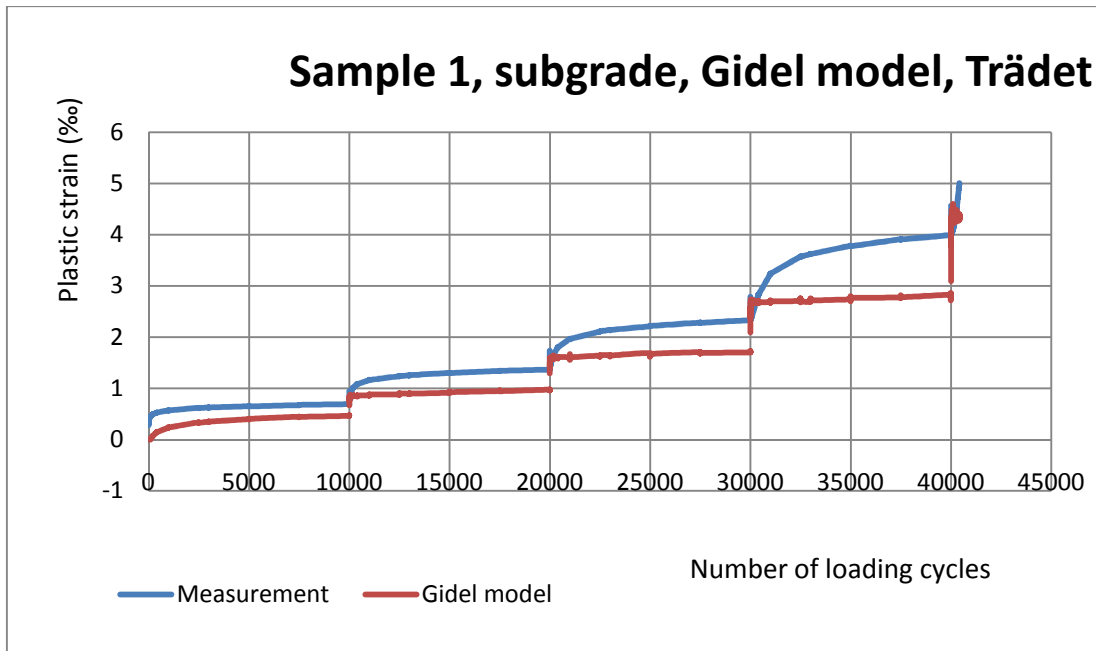


Figure 13.21 Gidel model factors calibrations with RLT data, sample 1, subgrade, Trädet.

Sample 2

Table 13.20 Shakedown range evaluation result for sample 2, subgrade, Trädet.

Sequence	Number of loading cycles	Confining pressure (kPa)	Deviatoric pressure (kPa)	Shakedown range
0	10000	20	50	A
1	10000	20	80	A
2	10000	20	110	B
3	10000	20	140	B
4	890	20	170	-

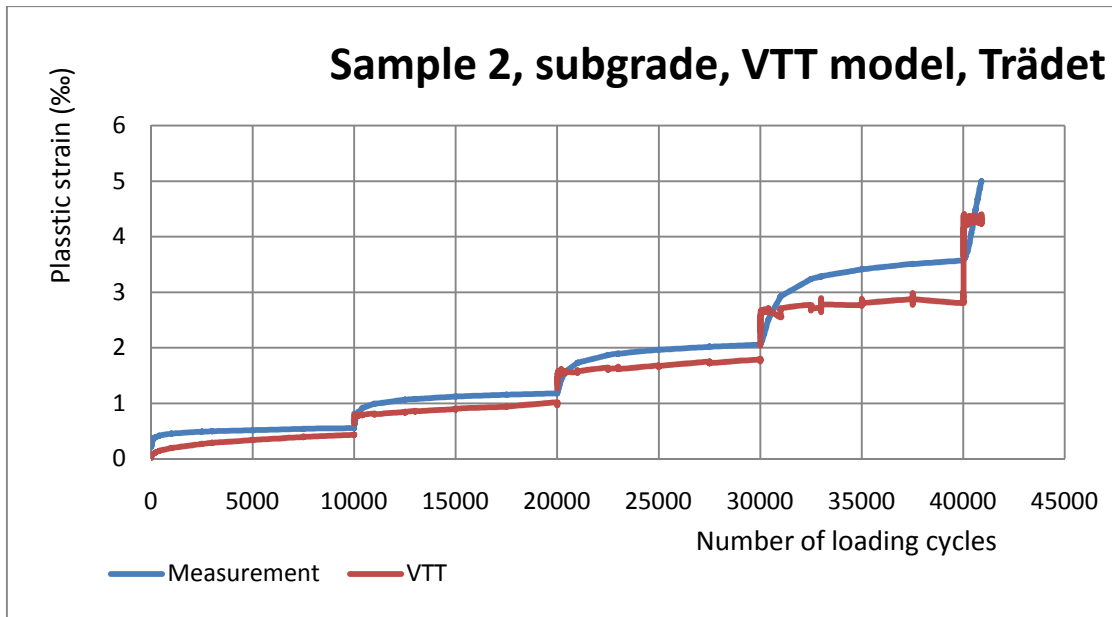


Figure 13.22 VTT model factors calibrations with RLT data, sample 2, subgrade, Trädet.

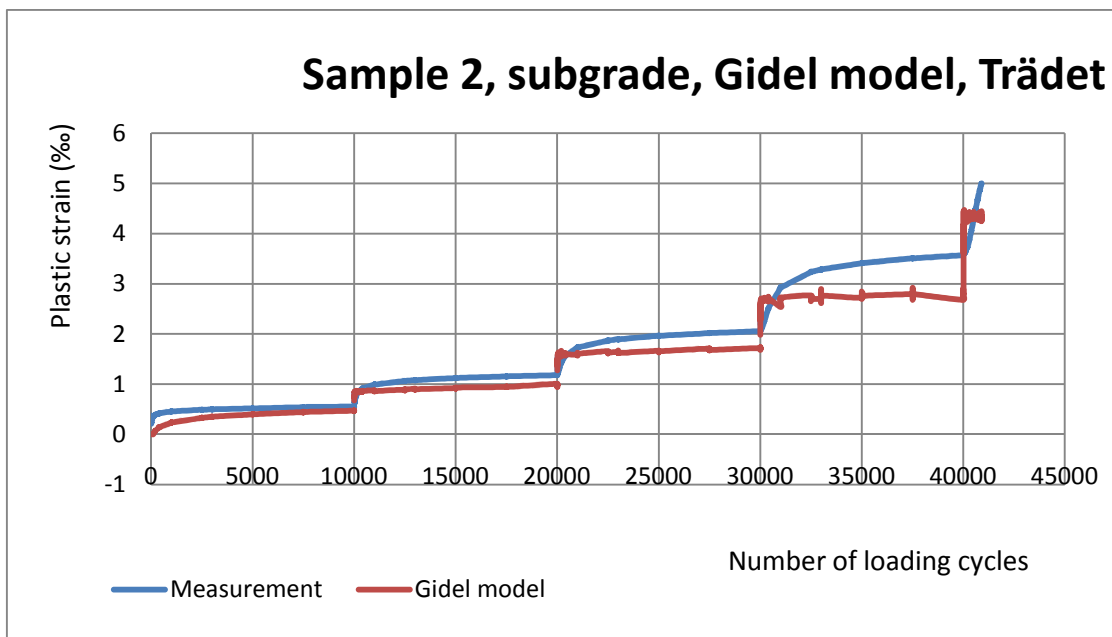


Figure 13.23 Gidel model factors calibrations with RLT data, sample 2, subgrade, Trädet.

Sample 3

Table 13.21 Shakedown range evaluation result for sample 3, subgrade, Trädet.

Sequence	Number of loading cycles	Confining pressure (kPa)	Deviatoric pressure (kPa)	Shakedown range
0	10000	20	50	A
1	10000	20	80	A
2	10000	20	110	B
3	10000	20	140	B
4	632	20	170	-

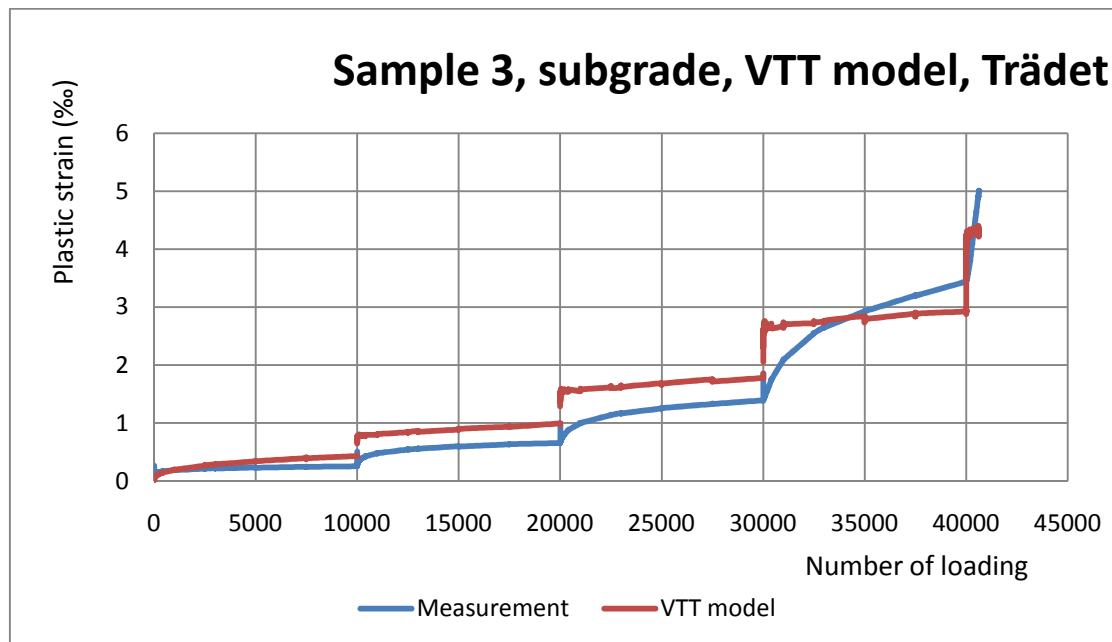


Figure 13.24 VTT model factors calibrations with RLT data, sample 3, subgrade, Trädet.

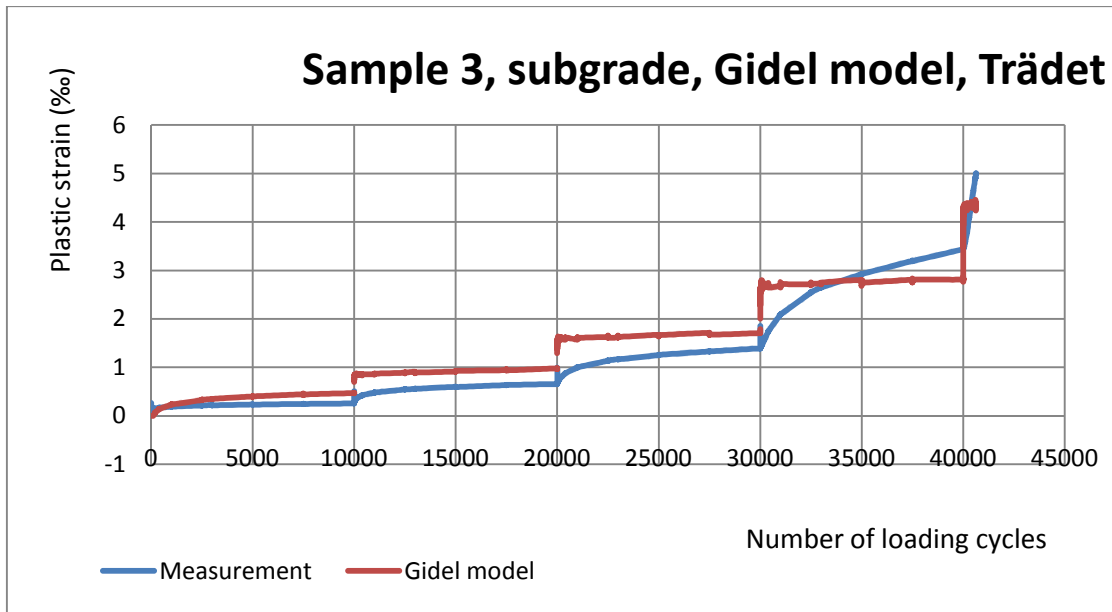


Figure 13.25 Gidel model factors calibrations with RLT data, sample 3, subgrade, Trädet.

Sample 4

Table 13.22 Shakedown range evaluation result for sample 4, subgrade, Trädet.

Sequence	Number of loading cycles	Confining pressure (kPa)	Deviatoric pressure (kPa)	Shakedown range
0	10000	20	20	A
1	10000	20	40	A
2	10000	20	60	A
3	10000	20	80	B
4	10000	20	100	B
5	10000	20	120	B

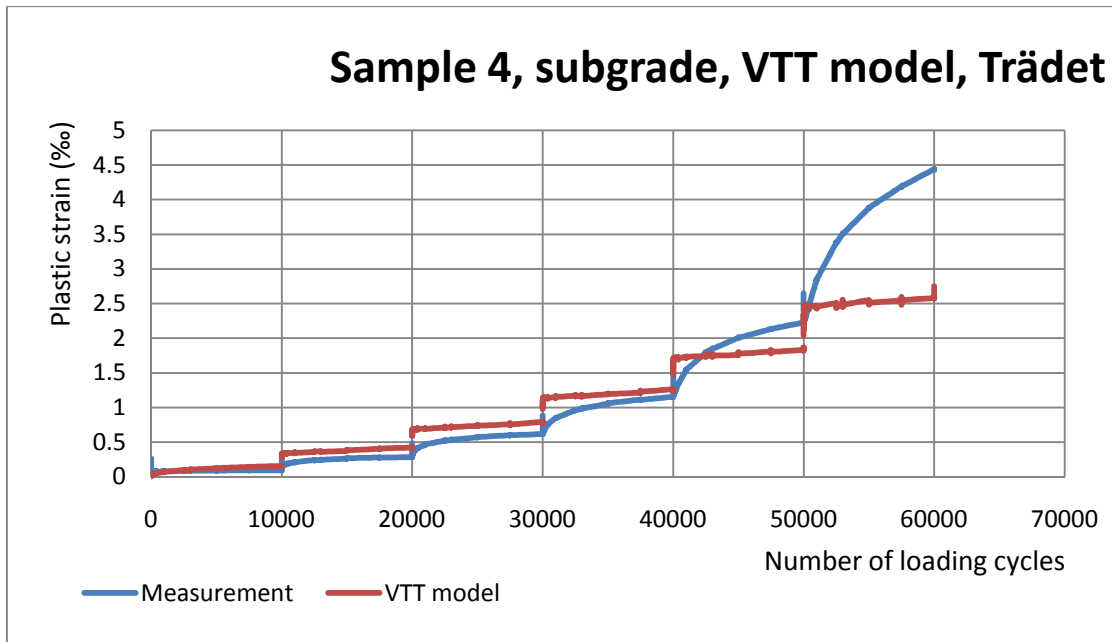


Figure 13.26 VTT model factors calibrations with RLT data, sample 4, subgrade, Trädet.

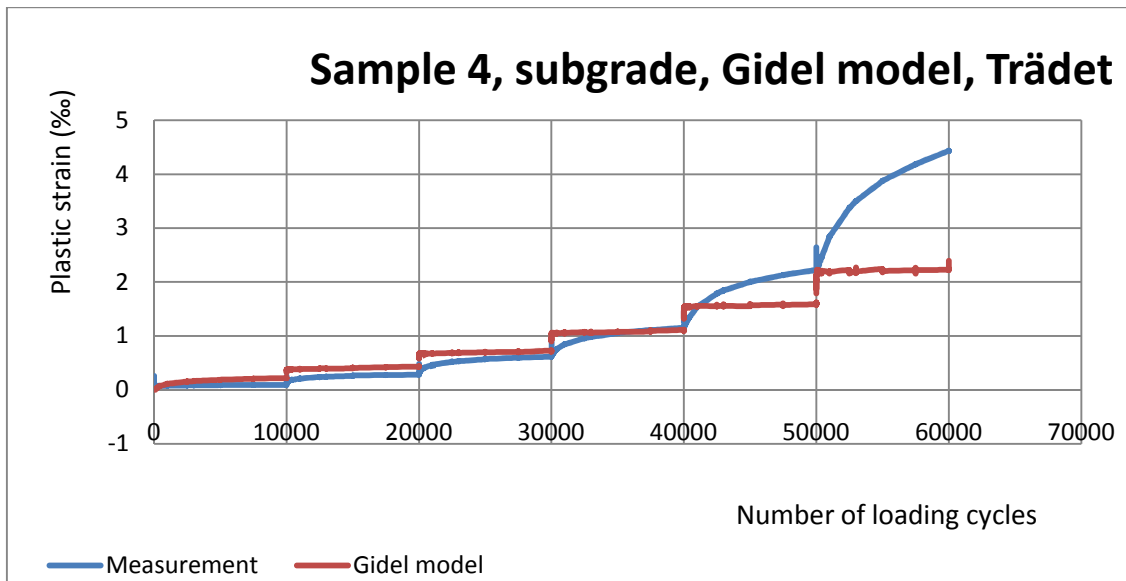


Figure 13.27 Gidel model factors calibrations with RLT data, sample 4, subgrade, Trädet.

12.2 Appendix 2

The measurement of rut depth has been done around every second year. The measurement has been inputted into the LTPP data base. RST car equipped with 17 lasers has been used in the measurement.

Dingle

Table 13.23 Rut depth measurement data in Dingle.

Year	2001	2002	2003	2004	2005	2006	2007	2008
Rutting depth (mm)	3	4.5	7	9.6	12.2	14.8	17.4	20

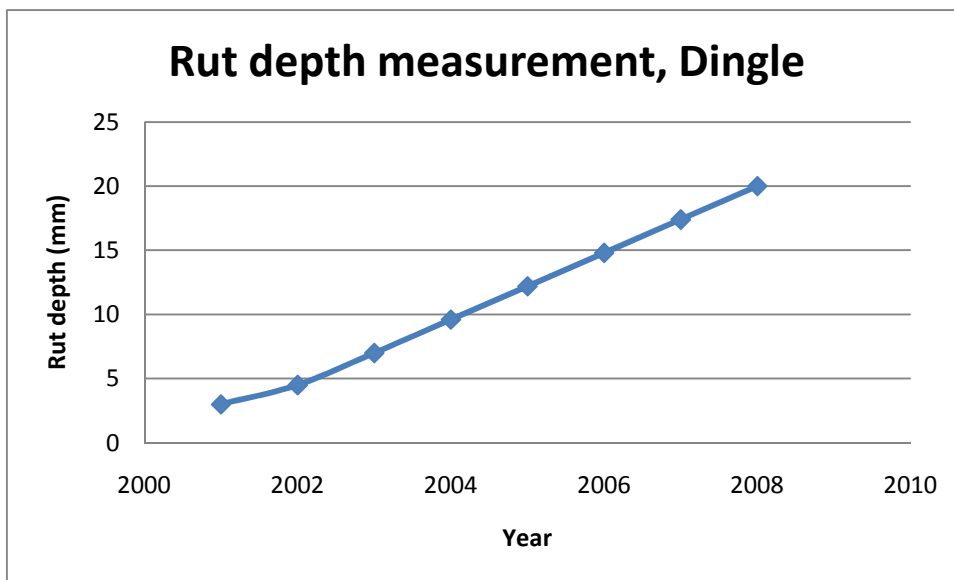


Figure 13.28 Rut depth measurements in Dingle.

The information about rut depth in Dingle is available in NordFoU project (Performance Prediction Models for Flexible Pavements, Part 2; Project level, Draft version, 2009). It shows clear evidence that the rut depth has been increasing fast in the past ten years.

Nässjö

Table 13.24 Rut depth measurement data in Nässjö.

Year	1997	1998	1999	2000	2002	2004
Max rut depth(mm)	9.8	10.4	11.6	12.6	14.4	16.8
Min rut depth (mm)	6.1	4.7	6.9	7.2	8.3	9.5

Mean rut depth (mm)	7.95	7.55	9.25	9.9	11.35	13.15
---------------------	------	------	------	-----	-------	-------

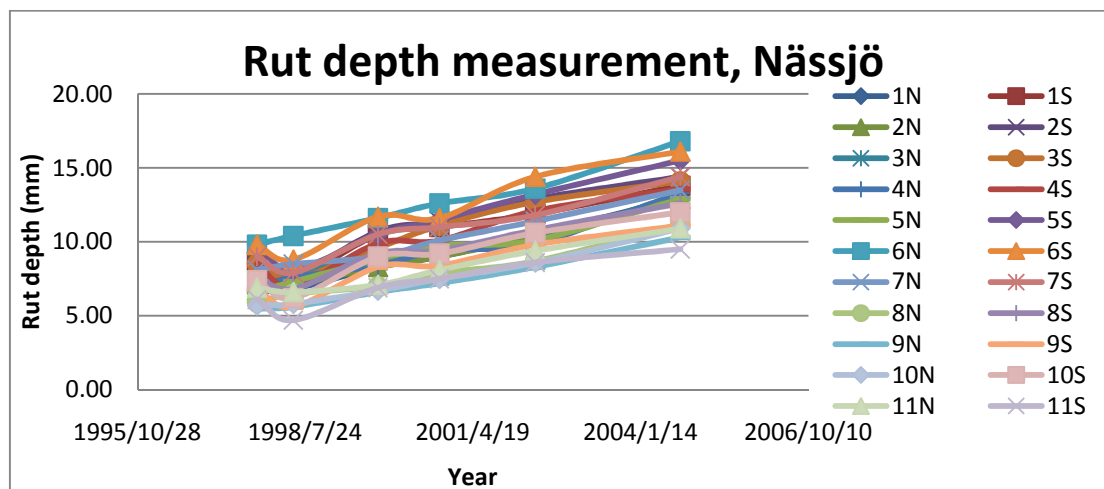


Figure 13.29 Rut depth measurements in Nässjö.

In LTPP database, there is rut measurement for all eleven sections from Nässjö. Although the traffic and weather condition is identical in those sections, variant in rut depth exists because of the difference in geometry of the section and in- situ condition (e.g. shadows from surrounding trees). The maximum rut depth takes place in section 6 and in section 11 the minimum rut depth occurs.

Trädet

Table 13.25 Rut depth measurement data in Trädet.

Year	1998	1999	2000	2002	2004
Max rut depth (mm)	8.7	10.7	11.5	13.3	16
Min rut depth (mm)	2.9	4.3	4.2	4.8	5.3
Mean rut depth (mm)	5.8	7.5	7.85	9.05	10.65

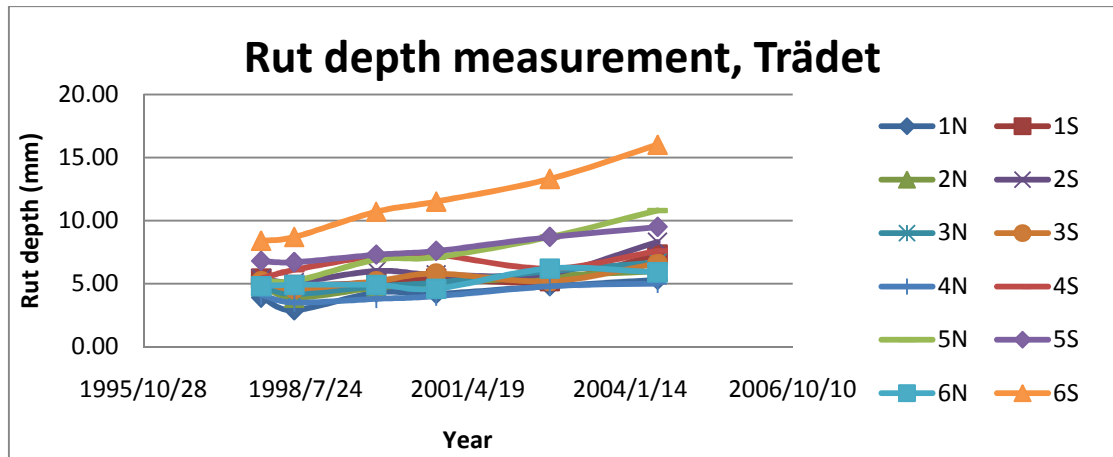


Figure 13.30 Rut depth measurements in Trädet.

The rutting from Trädet is smallest on all three roads. The maximum rut happens on section 6 while the minimum rut depth appears on section 1.

12.3 Appendix 3

Table 13.26 Temperature distribution in Dingle throughout one year.

Dingle	Temperature (°C)	Temperature distribution (%)
	20	95
	30	5

For Dingle, there are only 2 temperatures for VägFEM input files without the temperature distribution. An assumption is made as 95% days in a year is with temperature 20 °C while the rest 5% days are with 30 °C.

Table 13.27 Temperature distribution in Nässjö throughout one year.

Nässjö	Temperature (°C)	Temperature distribution (%)
	3	22
	8	22
	13	17.8
	18	20
	23	9.9
	28	5.8
	33	1.9
	38	0.6

Table 13.28 Temperature distribution in Trädet throughout one year.

Trädet	Temperature (°C)	Temperature distribution (%)
	0	50
	10	20
	20	20
	27	8
	35	2

12.4 Appendix 4

The traffic data are from LTPP database. The original data includes number of cars, heavy vehicles and axle information. The equivalent single axle loads calculated exclusively from heavy vehicles by multiplying the number of heavy vehicles and equivalent standard axles per heavy vehicle. The cumulative equivalent single axle loads (ESALs) are calculated by accumulating standard axles each year as time goes. The standard axle is equal to 10 ton here for designing purpose. Need to be specified that cumulative ESALs which is going to be filled in VägFEM as number of loading repetitions is required to approximate to the closest one thousand.

Dingle

Table 13.29 Traffic condition (cumulative ESALs) in Dingle.

Location	Road section	Cumulative ESALs
Dingle	E 6	
	Year	
	2001	552000
	2002	859000
	2003	1189000
	2004	1531000
	2005	1884000
	2006	2249000
	2007	2627000
	2008	3019000

Calculation starts from the year 2000 when the road is open to public. From 2000 to 2003, the growth in the traffic is 7.40 % from calculation while from the year 2003, the growth rate decreases to 3.47 %.

Nässjö

Table 13.30 Traffic condition (cumulative ESALs) in Nässjö.

Location	Road section	Cumulative ESALs
Nässjö	Rv 31	
	Year	
	1997	1100000
	1998	1217000
	1999	1336000
	2000	1456000
	2002	1701000
	2004	1952000

Calculation of cumulative ESAL starts from the year 1988 when traffic has been loading on the road. The traffic growth is set to be 1.2 % from the beginning until the end.

Trädet

Table 13.31 Traffic condition (cumulative ESALs) in Trädet.

Location	Road section	Cumulative ESALs
Trädet	Rv 46	
	Year	
	1998	788000
	1999	860000
	2000	932000
	2002	1079000
	2004	1230000

The road was completed by November in 1986 while the remaining December in that year is too short to be considered as one year. So calculation starts from 1987. The traffic growth is 1.3 % each year.

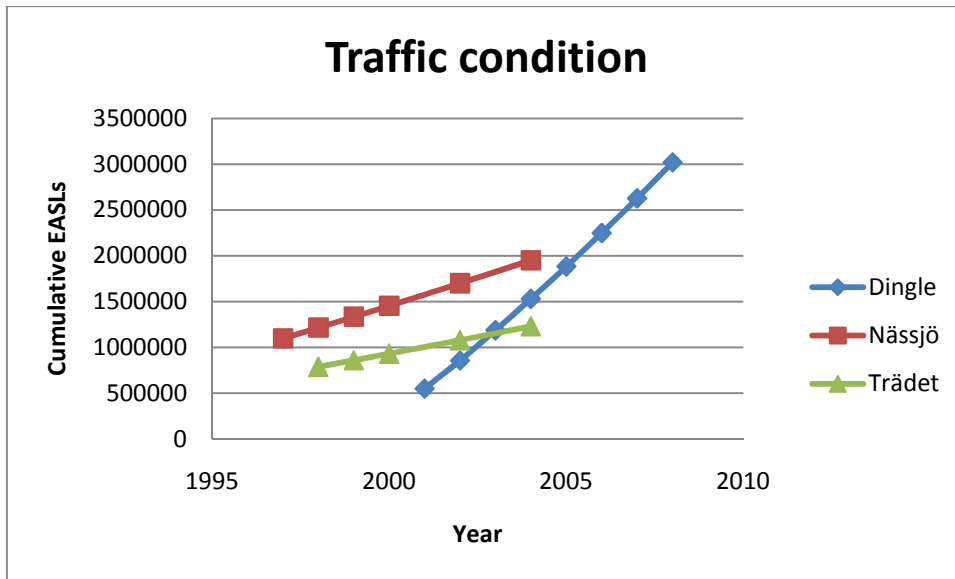


Figure 13.31 Traffic volume comparisons.

It can be seen that the traffic growth in Dingle is much faster than that in Nässjö or Trädet. The traffic growth in Nässjö and Trädet are very close, which is about 1 percent each year while Nässjö has almost twice as much cumulative ESALs passed than Trädet.

13 List of figures

- Figure 2.1 Location of Dingle and road Rv E6 (Huvstig 09).
- Figure 2.2 Location of Nässjö and road Rv 31 (Huvstig 09).
- Figure 2.3 Location of Trädet and road Rv 46 (Huvstig 09).
- Figure 3.1 Multi-layer system of a pavement.
- Figure 3.2 A picture illustrating a rut.
- Figure 3.3 Clearly sorted shakedown range by plotting vertical permanent strain rate and vertical permanent strain.
- Figure 3.4 Shakedown ranges plotted on a ϵ_p versus N diagram.
- Figure 4.1 The multi-layer model for calculating rutting depth.
- Figure 5.1 Relation between vertical strain and q/q_f .
- Figure 5.2 An example of static tests result.
- Figure 5.3 Phases described in MMOPP model (Hildebrand 2007).
- Figure 6.1 Stresses imposed on a sample in triaxial test.
- Figure 7.1 Shakedown range analysis.
- Figure 7.2 Factor calibrations for Sample 4, D1, Dingle.
- Figure 7.3 Comparisons between measured rut, VTT model prediction and Gidel model prediction for Dingle.
- Figure 7.4 Comparisons between measured rut, VTT model prediction and Gidel model prediction for Nässjö.
- Figure 7.5 Comparisons between measured rut, VTT model prediction and Gidel model prediction for Trädet.
- Figure 8.1 Sensitivity analysis.
- Figure 13.1 VTT model factors calibrations with RLT data, sample 1, Base, Dingle.
- Figure 13.2 VTT model factors calibrations with RLT data, sample 3, Base, Dingle.
- Figure 13.3 VTT model factors calibrations with RLT data, sample 4, Base, Dingle.
- Figure 13.4 VTT model factors calibrations with RLT data, sample 1, Base, Nässjö.
- Figure 13.5 VTT model factors calibrations with RLT data, sample 2, base, Nässjö.
- Figure 13.6 VTT model factors calibrations with RLT data, sample 3, base, Nässjö.
- Figure 13.7 VTT model factors calibrations with RLT data, sample 4, base, Nässjö.
- Figure 13.8 VTT model factors calibrations with RLT data, sample 5, base, Nässjö.
- Figure 13.9 VTT model factors calibrations with RLT data, sample 1, subbase, Nässjö.
- Figure 13.10 VTT model factors calibrations with RLT data, sample 2, subbase, Nässjö.
- Figure 13.11 VTT model factors calibrations with RLT data, sample 3, subbase, Nässjö.

Figure 13.12 VTT model factors calibrations with RLT data, sample 4, subbase, Nässjö.

Figure 13.13 VTT model factors calibrations with RLT data, sample 1, subgrade, Nässjö.

Figure 13.14 VTT model factors calibrations with RLT data, sample 2, subgrade, Nässjö.

Figure 13.15 Gidel model factors calibrations with RLT data, sample 2, subgrade, Nässjö.

Figure 13.16 VTT model factors calibrations with RLT data, sample 3, subgrade, Nässjö.

Figure 13.17 VTT model factors calibrations with RLT data, sample 4, subgrade, Nässjö.

Figure 13.18 VTT model factors calibrations with RLT data, sample 1, base, Trädet.

Figure 13.19 VTT model factors calibrations with RLT data, sample 2, base, Trädet.

Figure 13.20 VTT model factors calibrations with RLT data, sample 1, subgrade, Trädet.

Figure 13.21 Gidel model factors calibrations with RLT data, sample 1, subgrade, Trädet.

Figure 13.22 VTT model factors calibrations with RLT data, sample 2, subgrade, Trädet.

Figure 13.23 Gidel model factors calibrations with RLT data, sample 2, subgrade, Trädet.

Figure 13.24 VTT model factors calibrations with RLT data, sample 3, subgrade, Trädet.

Figure 13.26 VTT model factors calibrations with RLT data, sample 4, subgrade, Trädet.

Figure 13.27 Gidel model factors calibrations with RLT data, sample 4, subgrade, Trädet.

Figure 13.28 Rut depth measurements in Dingle.

Figure 13.29 Rut depth measurements in Nässjö.

Figure 13.30 Rut depth measurements in Trädet.

Figure 13.31 Traffic volume comparisons.

14 List of tables

- Table 2.1 Layer information of tested section, Rv E6,Dingle (Huvstig 09).
- Table 2.2 Layer information of Section 6S and 9S, Rv 31, Nässjö (Huvstig 09).
- Table 2.3 Layer information of Section 4, Rv 46, Trädet (Huvstig 09).
- Table 2.4 Sample condition.
- Table 7.1 Shakedown range analysis of Sample 1, Dingle
- Table 7.2 Shakedown limit line, creep limit line and static failure line information.
- Table 7.3 Calibrated factor for VTT model.
- Table 7.4 Calibrated factor for Gidel model.
- Table 13.1 Shakedown range evaluation result for sample 1, base, Dingle.
- Table 13.2 Shakedown range evaluation result for sample 3, base, Dingle.
- Table 13.3 Shakedown range evaluation result for sample 4, base, Dingle.
- Table 13.4 Shakedown range evaluation result for sample 1, base, Nässjö.
- Table 13.5 Shakedown range evaluation result for sample 2, base, Nässjö.
- Table 13.6 Shakedown range evaluation result for sample 3, base, Nässjö.
- Table 13.7 Shakedown range evaluation result for sample 4, base, Nässjö.
- Table 13.8 Shakedown range evaluation result for sample 5, base, Nässjö.
- Table 13.9 Shakedown range evaluation result for sample 1, subbase, Nässjö.
- Table 13.10 Shakedown range evaluation result for sample 2, subbase, Nässjö.
- Table 13.11 Shakedown range evaluation result for sample 3, subbase, Nässjö.
- Table 13.12 Shakedown range evaluation result for sample 4, subbase, Nässjö.
- Table 13.13 Shakedown range evaluation result for sample 1, subgrade, Nässjö.
- Table 13.14 Shakedown range evaluation result for sample 2, subgrade, Nässjö.
- Table 13.15 Shakedown range evaluation result for sample 3, subgrade, Nässjö.
- Table 13.16 Shakedown range evaluation result for sample 4, subgrade, Nässjö.
- Table 13.17 Shakedown range evaluation result for sample 1, base, Trädet.
- Table 13.18 Shakedown range evaluation result for sample 2, base, Trädet.
- Table 13.19 Shakedown range evaluation result for sample 1, subgrade, Trädet.
- Table 13.20 Shakedown range evaluation result for sample 2, subgrade, Trädet.
- Table 13.21 Shakedown range evaluation result for sample 3, subgrade, Trädet.
- Table 13.22 Shakedown range evaluation result for sample 4, subgrade, Trädet.
- Table 13.23 Rut depth measurement data in Dingle.
- Table 13.24 Rut depth measurement data in Nässjö
- Table 13.25 Rut depth measurement data in Trädet.
- Table 13.26 Temperature distribution in Dingle throughout one year.

Table 13.27 Temperature distribution in Nässjö throughout one year.

Table 13.28 Temperature distribution in Trädet throughout one year.

Table 13.29 Traffic condition (cumulative EASLs) in Dingle.

Table 13.30 Traffic condition (cumulative EASLs) in Nässjö.

Table 13.31 Traffic condition (cumulative ESALs) in Trädet.

